Journal of Medicinal Chemistry

pubs.acs.org/jmc Article

EEDi-5285: An Exceptionally Potent, Efficacious, and Orally Active Small-Molecule Inhibitor of Embryonic Ectoderm Development

Rohan Kalyan Rej,[▽] Changwei Wang,[▽] Jianfeng Lu, Mi Wang, Elyse Petrunak, Kaitlin P. Zawacki, Donna McEachern, Ester Fernandez-Salas, Chao-Yie Yang, Lu Wang, Ruiting Li, Krishnapriya Chinnaswamy, Bo Wen, Duxin Sun, Jeanne Stuckey, Yunlong Zhou, Jianyong Chen, Guozhi Tang, and Shaomeng Wang*

Cite This: J. Med. Chem. 2020, 63, 7252−7267 Read Online

ACCESS | Metrics & More | Article Recommendations | Supporting Information

ABSTRACT: Inhibition of embryonic ectoderm development (EED) is a new cancer therapeutic strategy. Herein, we report our discovery of EEDi-5285 as an exceptionally potent, efficacious, and orally active EED inhibitor. EEDi-5285 binds to the EED protein with an IC_{50} value of 0.2 nM and inhibits cell growth with IC_{50} values of 20 pM and 0.5 nM in the Pfeiffer and KARPAS422 lymphoma cell lines, respectively, carrying an EZH2 mutation. EEDi-5285 is approximately 100 times more potent than EED226 in binding to EED and >300 times more potent than EED226 in inhibition of cell growth in the KARPAS422 cell line. EEDi-5285 has excellent pharmacokinetics and achieves complete and durable tumor regression in the KARPAS422 xenograft model in mice with oral administration. The cocrystal structure of EEDi-5285 in a complex with EED defines the precise structural basis for their high binding affinity. EEDi-5285 is the most potent and efficacious EED inhibitor reported to date.

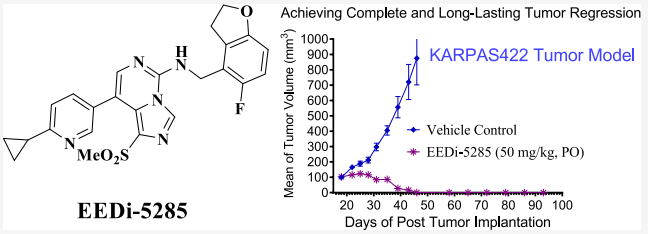

INTRODUCTION

The polycomb group (PcG) is a family of proteins responsible for cellular differentiation during development via transcriptional repression.[1,2] In mammals, PcG proteins are part of two major transcriptionally repressive complexes known as polycomb-repressive complexes 1 and 2 (PRC1 and PRC2).[3,4] The core PRC2 complex is composed of three proteins: the catalytic subunit EZH2 (an enhancer of zeste homolog 2), EED (embryonic ectoderm development), and SUZ12 (suppressor of zeste 12). PRC2 acts as an epigenetic modulator of transcription and plays a major role in a variety of biological processes, such as stem-cell maintenance and DNA repair.[5]

EZH2 is one of the most extensively studied histone methyltransferases, which catalyzes methylation of histone 3 lysine 27 (H3K27). In order to be catalytically active, EZH2 requires, at a minimum, two other PRC2 components, EED and SUZ12. EED enhances the enzymatic activity of PRC2 by binding with trimethylated H3K27 (H3K27me3), and SUZ12 interacts with other subunits within the PRC2 complex and contributes to the stability of the complex.[6,7] By binding directly with H3K27me3, EED localizes the PRC2 complex to the chromatin substrate and allosterically activates the methyltransferase activity.[8,9] The absence of either SUZ12 or EED completely abrogates the PRC2 function.[10]

Because the dysregulation of the PRC2 activity has been firmly linked to several forms of human cancers, major efforts have been made to develop small-molecule inhibitors targeting the PRC2 activity. One approach is to develop small-molecule inhibitors that directly bind to and inhibit EZH2, and this has yielded several EZH2 inhibitors such as compounds **1**−**3** (Figure 1), which are currently in clinical trials.[11−14] Tazemetostat (**2**) was approved in January 2020 by the US FDA for the treatment of advanced epithelioid sarcoma as a monotherapy.

Although inhibitors of EZH2 have shown promising clinical activity, preclinical data suggest that resistance can be acquired through secondary mutations in EZH2.[15] Consequently, targeting the allosteric site within the regulatory EED subunit of PRC2 offers a novel therapeutic strategy to target the PRC2 activity.[8,9] Scientists from Novartis[8] and AbbVie[9] first reported small-molecule inhibitors of the PRC2 activity, which function by targeting the histone-binding pocket in EED. Preclinical studies have shown that EED inhibitors such as EED226 (**4**), A-395 (**5**), and BR-001 (**6**) achieve strong antitumor activity in an EZH2 mutant lymphoma model as well as in EZH2

Received: March 21, 2020
Published: June 24, 2020

https://dx.doi.org/10.1021/acs.jmedchem.0c00479
J. Med. Chem. 2020, 63, 7252−7267

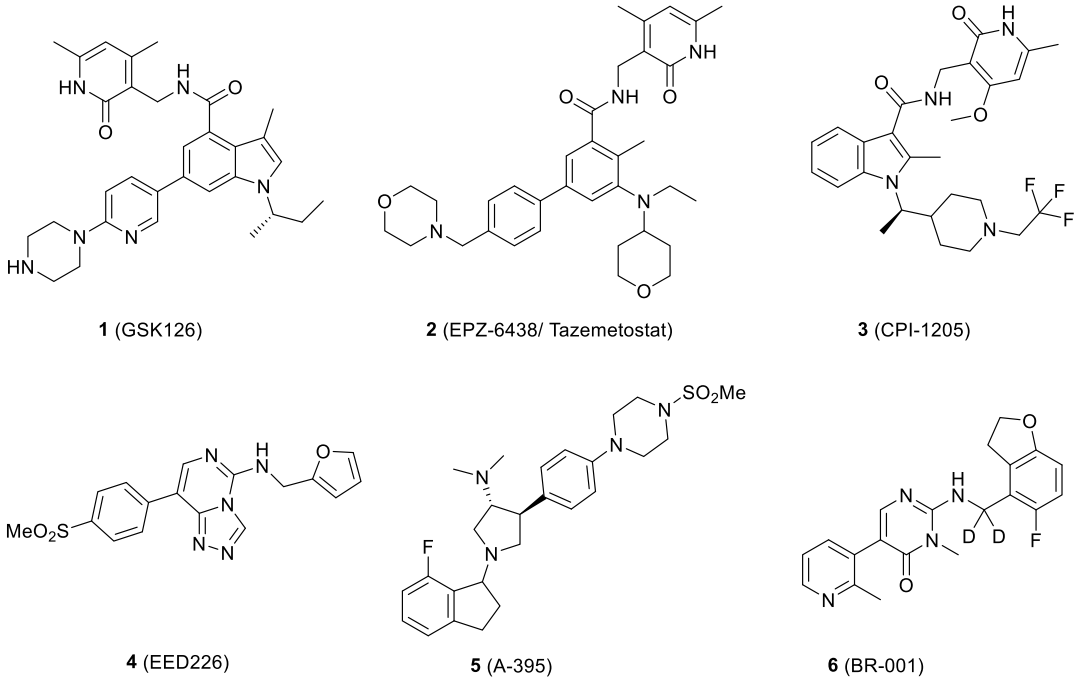

Figure 1. Representative small-molecule inhibitors of EZH2 and EED that target the PRC2 activity.

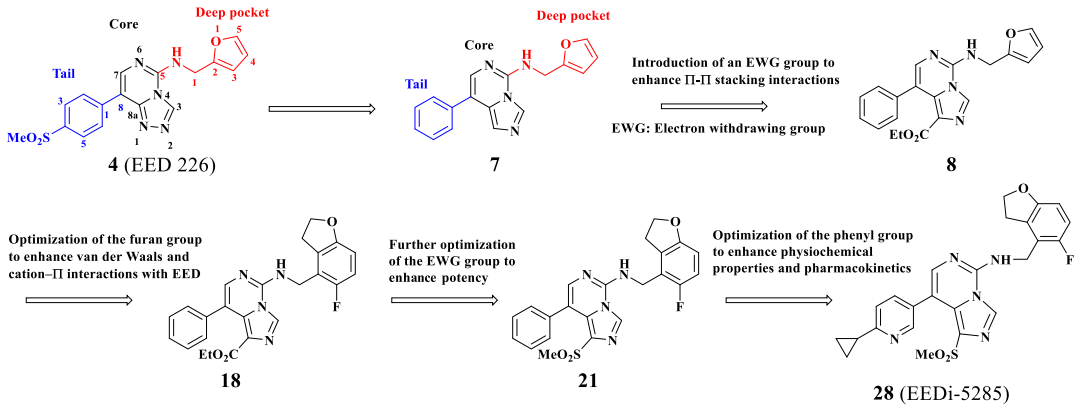

Figure 2. Structure-guided design and optimization of new EED inhibitors.

inhibitor-resistant models.[8,9,16−18] To date, MAK683, a small-molecular EED inhibitor developed by Novartis, is the only EED inhibitor that has advanced into Phase1/2 clinical trials for advanced malignancies (https://clinicaltrials.gov/ct2/-show/NCT02900651). The chemical structure and the preclinical and clinical data for MAK683 have not been disclosed.

Herein, we report our structure-guided discovery of small-molecule inhibitors of EED. Our efforts have yielded the discovery of EEDi-5285 as an exceptionally potent, efficacious, and orally active small-molecule inhibitor of EED, which achieves complete and long-lasting tumor regression in mice. EEDi-5285 is the most potent and efficacious EED inhibitor reported to date.

RESULTS AND DISCUSSION

The starting point for our design is based upon the cocrystal structure of EED226 (**4**) in a complex with EED (PDB accession code: 5GSA).[8,16] The cocrystal structure shows that the furan unit in EED226 inserts deeply into an aromatic "cage" formed by four aromatic residues. The electron-deficient bicyclic [1,2,4]triazolo[4,3-*c*]pyrimidine core of EED226 forms $\pi-\pi$ stacking interactions with the electron-rich Tyr148 and Tyr365 residues of EED. The electron-rich furan of EED226 has cation$-\pi$ interactions with the guanidinium group of Arg367 of EED and an edge-to-face interaction with Tyr365 of EED. EED226 is also stabilized by two hydrogen bonds with EED: the amino group linking the bicyclic core and the furan group form a hydrogen bond with the side chain carbonyl oxygen of Asn194, and N2 of the triazolopyrimidine core forms a hydrogen bond with the side chain of Lys211. The methylsulfonylphenyl group is mostly exposed to solvents but its methyl group interacts with Pro95 and its phenyl group enjoys an edge-to-face interaction with the side chain of Phe97.

For our design of EED inhibitors, we used compound 7 (Figure 2),[15] a previously reported, moderately potent EED inhibitor as the starting point for our optimization efforts based on the following considerations: (a) 7 has a good binding affinity to EED with IC_{50} = 115 nM in our assay (Table 1); (b) 7 is cell-permeable and shows an inhibitory activity in KARPAS422 lymphoma cell lines with IC_{50} = 2.6 μM (Table

https://dx.doi.org/10.1021/acs.jmedchem.0c00479
J. Med. Chem. 2020, 63, 7252−7267

Table 1. Investigation of the Effect of an EWG on the Imidazo[1,5-*c*]pyrimidine Core in Compound 7

Compd.	Structure	Binding to EED (IC_{50}, nM)	Cell growth inhibition in KARPAS422 (IC_{50}, μM)
EED226		17.6 ± 5.8	0.18 ± 0.05
7	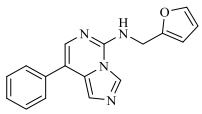	115 ± 24	2.6 ± 0.4
8	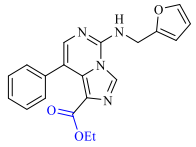	59 ± 8	1.0 ± 0.1
9	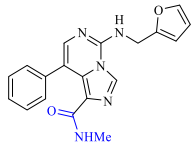	92 ± 7	2.4 ± 0.4

1); (c) the published cocrystal structure of EED226 complexed with EED provides a foundation for the structure-guided optimization shown in Figure 2.

We sought to improve the binding affinity of compound **7** to EED. Compared to the electron-deficient bicyclic [1,2,4]-triazolo[4,3-*c*]pyridine core in EED226, the imidazo[1,5-*c*]pyrimidine core in compound **7** is more electron-rich. We hypothesized that the binding affinity of compound **7** to EED may be improved by installation of an electron-withdrawing group onto its imidazo[1,5-*c*]pyrimidine core to enhance its $\pi-\pi$ stacking interactions with the electron-rich Tyr148 and Tyr365 residues of EED. Accordingly, we synthesized compounds **8** and **9** and tested their binding affinity to EED and their cell growth inhibitory activity in the KARPAS422 cell line (Table 1). While **9** with a methylamide group has a binding affinity similar to that of **7**, compound **8** containing an ethyl ester group is 2 times more potent than **7** in binding to EED and in inhibition of cell growth in KARPAS422 cells (Table 1). In our assays, EED226 has an IC_{50} value of 17.6 nM in its binding to EED and an IC_{50} value of 0.18 μM in inhibition of cell growth in the KARPAS422 cell line. We employed compound **8** as the new lead compound for further optimization.

Because the furan group in compound **8** is metabolically liable,[19] we next synthesized and tested a number of compounds by replacing the furan group with other aromatic rings, with the results summarized in Table 2. Replacement of the furan with a phenyl group yielded compound **10**, which is 2−3 times less potent than compound **8** in both binding and cellular assays. To enhance the cation$-\pi$ interactions with the guanidinium group of Arg367 of EED, an electron-rich 2-methoxy group was introduced onto the phenyl group of **10**, generating compound **11**. Compound **11** has an IC_{50} of 86 nM in binding to EED and an IC_{50} value of 1.9 μM in cell growth inhibition in KARPAS422 cells and thus is slightly more potent than **10**. Installation of a fluorine substituent at the C6 in the 2-methoxyphenyl ring of **11** yielded **12**, which binds to EED

Table 2. Investigation of SAR by Replacing the Metabolically Labile Furan Ring

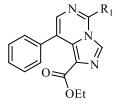

Compd.	R_1	Binding to EED (IC_{50}, nM)	Cell growth inhibition in KARPAS422 (IC_{50}, μM)
10	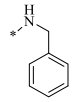	119 ± 24	3.0± 0.2
11	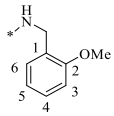	86 ± 6	1.9 ± 0.3
12	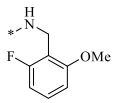	50 ± 3	0.3 ± 0.1
13	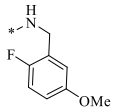	138 ± 9	2.7 ± 0.2
14	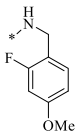	145 ± 0.3	4.3 ± 0.4
15	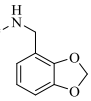	40 ± 4	0.3 ± 0.1
16	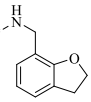	207 ± 0.5	6.3 ± 0.2
17	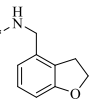	29 ± 0.1	0.21 ± 0.03
18	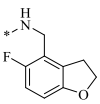	18 ± 1	0.012±0.01

with an IC_{50} value of 50 nM and achieves an IC_{50} value of 0.3 μM in inhibition of cell growth in KARPAS422 cells. Hence, although **12** is only slightly more potent than **11** in binding to EED, it is 6 times more potent than **11** in cell growth inhibition in KARPAS422 cells. Moving the methoxy group in compound **12** from C2 to C3 or C4 yielded compounds **13** and **14**, respectively. Compound **13** binds to EED with 138 nM and has an IC_{50} of 2.7 μM in KARPAS422 cells. Thus, **13** is 8 times less potent than **12** in cell growth inhibition in KARPAS422 cells. Compound **14** is slightly less potent than **13** in both binding and cellular assays.

https://dx.doi.org/10.1021/acs.jmedchem.0c00479
J. Med. Chem. 2020, 63, 7252−7267

Table 3. Further Optimization of the EWG Using 5-Fluoro-2,3-dihydrobenzofuran for the Deep Pocket

Compd.	Structures	Binding to EED (IC_{50}, nM)	Cell Growth Inhibition in KARPAS422 (IC_{50}, nM)
18	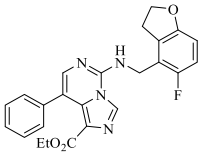	18 ± 1	12 ± 2
19	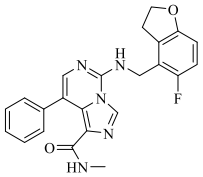	23 ± 1	60 ± 20
20	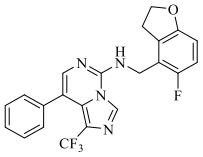	29 ± 2	120 ± 9
21	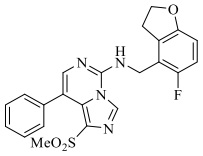	0.7 ± 0.3	2.2 ± 0.7
22	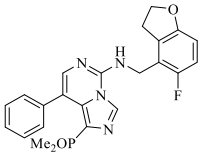	3.6 ± 1.2	8.1 ± 0.3

To further explore the deep binding pocket, we next synthesized a number of compounds containing an electron-rich bicyclic group to replace the phenyl group in **10**. Compound **15**, with a benzo[*d*][1,3]dioxole moiety, binds to EED with an IC_{50} value of 40 nM and achieves an IC_{50} of 0.3 μM in inhibition of KARPAS422 cell growth. Compounds **16** and **17** were prepared in an attempt to learn the preferred position of the oxygen atom. Compound **17** is 7 times more potent than **16** in binding to EED and 30 times more potent than **16** in inhibition of cell growth in the KARPAS422 cell line.

As introduction of a 6-fluoro substituent on the phenyl ring in **11** enhances the potency in both binding to EED and in cell growth inhibition, we installed a fluorine substituent at the same position in **17**, resulting in **18**. Compound **18** binds to EED with an IC_{50} value of 18 nM and potently inhibits KARPAS422 cell growth with an IC_{50} value of 12 nM. Hence, the 5-fluoro-2,3-dihydrobenzofuran group employed (Scheme 4) in **18**, which was previously disclosed in a Novartis patent application,[20] is the best among a number of groups investigated in our study.

Based upon the potent binding affinity of **18** to EED and its excellent cell growth inhibition in the KARPAS422 cell line, we performed further modifications of its ethyl ester electron-withdrawing group (EWG). Replacement of the ester group in **18** with a methylamide yielded compound **19**, which binds to EED with an IC_{50} value of 23 nM and inhibits KARPAS422 cell growth with an IC_{50} value of 60 nM. Replacing the ethyl ester with CF_3, a methylsulfone or a dimethylphosphine oxide yielded compounds **20**, **21**, and **22**, respectively. Compound **20** binds to EED with an IC_{50} value of 29 nM and inhibits KARPAS422 cell growth with an IC_{50} value of 120 nM. Compound **21**, containing a methylsulfone, achieves the best potency among this series of compounds, with IC_{50} = 0.7 nM to EED and IC_{50} = 2.2 nM in inhibition of KARPAS422 cell growth. Compound **22** achieves an IC_{50} value of 3.6 nM in binding to EED and an IC_{50} value of 8.1 nM in cell growth inhibition in the KARPAS422 cell line (Table 3).

In the cocrystal structure of EED226 complexed with EED, the phenyl group has interactions with Phe97 of EED and the methylsulfonyl group is largely exposed to a solvent. We next performed modifications of the corresponding phenyl group in compound **21**, with the results summarized in Table 4.

We first installed a 4-methylsulfonyl group in **21**, same as that in EED226 and obtained **23**, which binds to EED with an IC_{50} value of 0.4 nM and inhibits KARPAS422 cell growth with IC_{50} = 1.4 nM. Installation of a 4-fluoro substituent on the phenyl group of **21** resulted in **24**, which is slightly more potent than **21** in binding to EED (IC_{50} = 0.4 nM vs 0.7 nM) but is 2−3 times less potent than **21** in inhibition of KARPAS422 cell growth.

To improve the solubility of the compounds, we made a series of compounds in which the phenyl group in **21** was replaced with a pyridine. Compound **26** with a 2-methyl-3-pyridine group is half as potent as **21** in both binding to EED and inhibition of KARPAS422 cell growth. Compound **27** with a 4-methyl-3-pyridine group is slightly more potent than **21** in both binding to EED and inhibition of KARPAS422 cell growth. Compound **28** with a 4-cyclopropyl-3-pyridine substituent is 3−4 times more potent than **21** in both binding to EED and inhibition of KARPAS422 cell growth.

Encouraged by the results from compound **28**, we synthesized additional analogues with different substituents at the 4-position of the 3-pyridine group. Compound **29** with a difluoromethyl substituent binds to EED with IC_{50} = 0.2 nM, and is thus 5 times more potent than **21**, but its potency in inhibition of KARPAS422 cell growth is similar to that of **21**. Compound **30** with a trifluoromethyl group is slightly more potent than **21** in binding to EED and in inhibition of KARPAS422 cell growth. Compound **32** with 2,4-dimethyl-3-pyridine has a potency similar to that of **21** in both binding to EED and KARPAS422 cell growth inhibition. Compound **33** containing 2-methyl-4-trifluoromethyl-3-pyridine is slightly more potent than **21** in both binding to EED and cell growth inhibition of KARPAS422 cells.

We synthesized **34** by replacing the phenyl group in **21** with a 1-methyl-1*H*-pyrazole and found that these two compounds have a similar potency in binding to EED and in inhibition of KARPAS422 cell growth.

Because the 4-methylsulfonylphenyl group in EED226 has mainly hydrophobic contacts with EED, we synthesized a number of analogues by replacing the phenyl group in **21** with a nonaromatic, six-membered ring. Compound **35** with 4-tetrahydro-2*H*-pyran in place of this phenyl group binds to EED with IC_{50} = 12 nM, and is 17 times less potent than **21**. Consistent with its weaker binding affinity to EED, **35** is 24 times less potent than **21** in inhibition of KARPAS422 cell growth. Replacing the oxygen in the six-membered ring in **35** with sulfonyl, ethylamino, methylamide, methylsulfonylamide,

https://dx.doi.org/10.1021/acs.jmedchem.0c00479
J. Med. Chem. 2020, 63, 7252−7267

Table 4. Structure−Activity Relationship and Optimization of the Tail Part, R_2 at C8

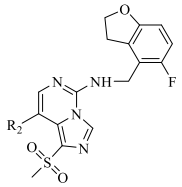

Compd.	R_2	Binding to EED IC_{50} (nM)	Cell Growth Inhibition in KARPAS422 Cells (IC_{50}, nM)	Cell Growth Inhibition in Pfeiffer Cells IC_{50} (nM)
21		0.7 ± 0.3	2.2 ± 0.7	NT
23	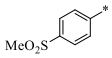	0.4 ± 0.2	1.4 ± 0.1	0.02 ± 0.01
24		0.4 ± 0.2	5.2 ± 0.2	0.12 ± 0.02
25	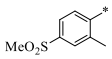	0.9 ± 0.2	1.6 ± 0.3	0.02 ± 0.01
26		1.8 ± 0.8	3.6 ± 0.4	0.08 ± 0.02
27		0.4 ± 0.3	1.4 ± 0.1	0.03 ± 0.05
28		0.2 ± 0.2	0.5 ± 0.1	0.02 ± 0.01
29	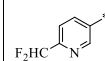	0.2 ± 0.1	2.4 ± 0.4	0.02 ± 0.05
30		0.3 ± 0.1	1.7 ± 0.1	0.03 ± 0.03
31	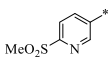	0.8 ± 0.5	2.9 ± 0.2	0.5 ±0.1
32		0.5 ± 0.2	2.8 ± 0.8	0.07 ± 0.03
33		0.4 ± 0.1	1.7± 0.6	0.05 ± 0.02
34		0.5 ± 0.2	3.1 ± 0.1	0.27 ± 0.15
35		12 ± 2	52 ± 1	NT
36		7.8 ± 1.4	29 ± 1	NT
37	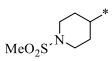	7.9 ± 2.0	15.3 ± 0.3	NT
38		23 ± 2	126 ± 1	NT
39		2.8 ± 1.6	6.5 ± 0.7	NT
40	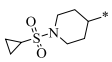	3.1 ± 1.2	8.2 ± 0.3	NT

NT = not tested.

or cyclopropylsulfonylamide generated compounds **36**−**40**, respectively. All of these compounds bind to EED with a weaker affinity than compound **21** and also show a weaker activity than **21** in inhibition of KARPAS422 cell growth.

In addition to the KARPAS422 cell line, the Pfeiffer lymphoma cell line, which carries an EZH2 mutation, is also very responsive to EED inhibitors.[9] We tested a number of representative compounds, which show potent cell growth inhibition in the KARPAS422 cell line, for their cell growth-inhibitory activity in the Pfeiffer cell line, obtaining the results summarized in Table 4.

Compounds with potent cell growth inhibition in the KARPAS422 cell line are generally more potent in the Pfeiffer cell line and a number of these compounds achieve picomolar potencies. For example, compounds **23**, **25**, **27**, **28**, **29**, and **30** achieve IC_{50} values of 20−30 pM in the Pfeiffer cell line. Thus, our modifications have produced a number of highly potent EED inhibitors, which bind to EED with subnanomolar affinities and have low nanomolar to subnanomolar IC_{50} values in inhibition of KARPAS422 cell growth and low picomolar IC_{50} values in inhibition of Pfeiffer cell growth.

Determination of Cocrystal Structures of EEDi-5285 and EEDi-1056 in a Complex with EED Protein. To define their precise binding modes and to understand the structural basis for their high affinity binding, we determined high-resolution cocrystal structures for EEDi-5285 (**28**) and EEDi-1056 (**32**) in a complex with EED (PDB ID: 6W7F and 6W7G, respectively).

For both EEDi-5285 and EEDi-1056, the 5-fluoro-2,3-dihydrobenzofuran group spatially fills the deep pocket of EED excluding all water molecules and engages in cation−π interactions with the guanidinium group of Arg367 of EED. This hand-in-glove style fit creates more van der Waals interactions with EED than furan group of EED226, which relies on transient waters for stabilization within the pocket. Although similar cation−π interactions are observed in the cocrystal structure of EED226 in a complex with EED (PDB accession code: 5GSA), the guanidinium group of Arg367 is not directly underneath the electron-rich furan group. In comparison, the guanidinium group of Arg367 is now directly underneath the 5-fluoro-2,3-dihydrobenzofuran group, suggesting stronger cation−π interactions than those observed in the EED226 cocrystal structure. In addition, the side chain of Tyr365 is directly above the benzo group of the 5-fluoro-2,3-dihydrobenzofuran group and enjoys more extensive interactions between them than those observed in the EED226 cocrystal structure. Similar to those observed in the EED226 cocrystal structure, there are π−π interactions between the 1-(methylsulfonyl)imidazo[1,5-*c*]pyrimidine core in both inhibitors and the two electron-rich Tyr148 and Tyr365 residues of EED, with the methylsulfonyl group exposed to the solvent environment. As compared to those observed in the EED226 cocrystal structure, there are also two similar hydrogen bonds formed between EED with either EEDi-5285 or EEDi-1056: a hydrogen bond between the amino group linking the 1-(methylsulfonyl)imidazo[1,5-*c*]pyrimidine core and the (5-fluoro-2,3-dihydrobenzofuran-4-yl)methyl group with the side chain carbonyl oxygen of Asn194 and another hydrogen bond between the N2 atom of the 1-(methylsulfonyl)imidazo[1,5-*c*]pyrimidine core and the side chain of Lys211. The 2-cyclopropylpyridinyl group in EEDi-5285 or 2,6-dimethylpyridinyl group in EEDi-1056 captures very similar interactions as the methylsulfonylphenyl group in EED226. These two cocrystal structures for EEDi-5285 and EEDi-1056 provide a

https://dx.doi.org/10.1021/acs.jmedchem.0c00479
J. Med. Chem. 2020, 63, 7252−7267

solid structural basis for their very high-affinity affinities with EED (Figure 3).

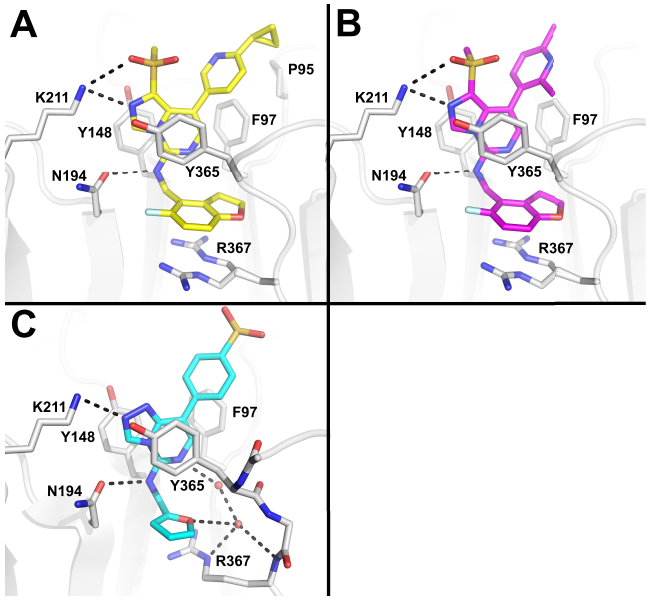

Figure 3. Cocrystal structures of EED bound to inhibitors. Key interactions of compound (a) EEDi-5285 with EED (PDB accession code 6W7F), (b) EEDi-1056 with EED (PDB accession code 6W7G) and (c) EED226 with EED (PDB accession code 5GSA) for comparison. Dashed lines represent hydrogen bonds. Water molecules are depicted as red spheres.

Interestingly, in both cocrystal structures, we also observed a secondary binding mode with an inhibitor molecule-bound EED opposite the primary, histone-binding pocket. In this secondary binding model, the 5-fluoro-2,3-dihydrobenzofuran group in both inhibitors fits into a relatively shallow pocket, with the rest of the molecule sitting on a large, surface pocket, suggesting low affinity interactions.

Pharmacokinetic Studies of EED Inhibitors in Mice. We evaluated 12 potent EED inhibitors (compounds **23**−**34**) in mice with three time-points to provide an initial assessment of their oral bioavailability obtaining the data summarized in Table 5.

The exposure data showed that a number of these EED inhibitors, such as **23**, **26**, **28**, **30**, and **32**, achieve good plasma concentrations, with **28** and **32** being the best.

Based on the initial oral exposure data, we selected compounds **28** and **32** for pharmacokinetic studies in mice and obtained the data summarized in Table 6. Compound **28** achieves a C_{max} of 1.8 μM and an AUC of 6.0 h*μg/ml with 10 mg/kg oral administration and has an oral bioavailability (F) of 75%. Compound **32** achieves a C_{max} of 1.3 μM and an AUC of 2.6 h* μg/ml with 10 mg/kg oral administration and has an oral bioavailability of 69%. Both compounds have a moderate volume of distribution of 1.4−1.6 L/kg and a terminal $T_{1/2}$ of approximately 2 h. The PK data thus show that both **28** and **32** have an excellent PK profile in mice.

Pharmacodynamic Studies of EED Inhibitors in KARPAS422 Tumor Tissue. We next evaluated compounds EEDi-5285 and EEDi-1056 for their pharmacodynamics (PD) effect in KARPAS422 tumor tissue in mice. Our PD data showed that a single 100 mg/kg oral administration of EEDi-5285 or EEDi-1056 effectively reduces the level of H3K27me3 at 24 h (Figure 4).

Table 5. Oral Exposure of EED Inhibitors in Plasma with Oral Administration in Mice[a]

	plasma drug concentration (ng/mL), PO (25 mg/kg)		
compound	1 h	3 h	6 h
23	598	171	109
24	43	<10	<10
25	591	279	98
26	488	194	91
27	340	94	29
28 (EEDi-5285)	1096	608	452
29	242	18	<10
30	468	189	139
31	351	36	41
32 (EEDi-1056)	2477	754	485
33	896	794	415
34	468	50	56

[a]Each compound was administered orally at 25 mg/kg. Plasma samples were collected at 1, 3, and 6 h with two mice at each time point and analyzed by LC−MS/MS. Mean values of drug concentrations are presented.

Antitumor Activity of EEDi-5285 and EEDi-1056 in the KARPAS422 Xenograft Model in Mice. We evaluated EEDi-5285 and EEDi-1056 for their antitumor activity in the KARPAS422 xenograft model in mice (Figure 5). Both compounds were administered 50 and 100 mg/kg via oral gavage, daily for 28 days. Both EEDi-5285 and EEDi-1056 achieved complete tumor regression at both 50 and 100 mg/kg during the treatment period (Figure 5A). Significantly, no regrowth of tumors was observed after treatment had been stopped for 72 days. Both the compounds caused minimal weight loss during the entire experiment (Figure 5B). This antitumor efficacy experiment demonstrated that both EEDi-5285 and EEDi-1056 are highly efficacious and capable of achieving complete and long-lasting tumor regression in the KARPAS422 xenograft model in mice with oral administration at well-tolerated dose schedules. As both EEDi-5285 and EEDi-1056 achieved complete tumor regression at 50 mg/kg, the lowest dose for them to achieve complete tumor regression in the KARPAS xenograft tumor model was not determined.

CHEMISTRY

Compounds **8**−**19** were prepared, as shown in Scheme 1, compounds **7** and **20**−**34** were prepared, as shown in Scheme 2, and compounds **35**−**40** were prepared, as shown in Scheme 3. Commercially available 5-bromo-4-chloro-2-(methylthio)-pyrimidine (compound **41**) was converted to the corresponding amine (**43**) by treatment with ethyl 2-(diphenylmethyleneamino)acetate, followed by acid-catalyzed hydrolysis. The amine (**43**) upon formylation followed by cyclization using $POCl_3$ afforded the bicyclic compound **45**, which was converted to **46** by selective displacement of the S−Me group with furan-2-ylmethanamine at the 5-position.[16] Using the Suzuki reaction conditions, compound **46** was converted to the phenyl analog (compound **8**). Target compounds **10**−**18** were made using this protocol with different amines, while compound **18** was obtained using 2-(7-azabenzotriazol-1-yl)-*N*,*N*,*N*′,*N*′-tetramethyluronium hexafluoro-phosphate (HATU) as the coupling reagent. The details

https://dx.doi.org/10.1021/acs.jmedchem.0c00479
J. Med. Chem. 2020, 63, 7252−7267

Table 6. Pharmacokinetic Parameters of 28 (EEDi-5285) and 32 (EEDi-1056) in Mice[a]

compd	route/dose	$T_{1/2}$ (h)	C_{max} (μg/mL)	AUC_{0-t} (h·μg/mL)	Cl (mL/min/kg)	V_{ss} (L/kg)	F (%)
28 (EEDi-5285)	IV/2 mg/kg			1.7	20	1.4	
	PO/10 mg/kg	2.0	1.8	6.0			75
32 (EEDi-1056)	IV/2 mg/kg			0.8	40	1.6	
	PO/10 mg/kg	2.1	1.3	2.6			69

[a] C_{max}, maximum drug concentration; AUC, area-under-the-curve; Cl = plasma clearance, V_{ss} = volume of distribution, $T_{1/2}$ = terminal half-life, F = oral bioavailability.

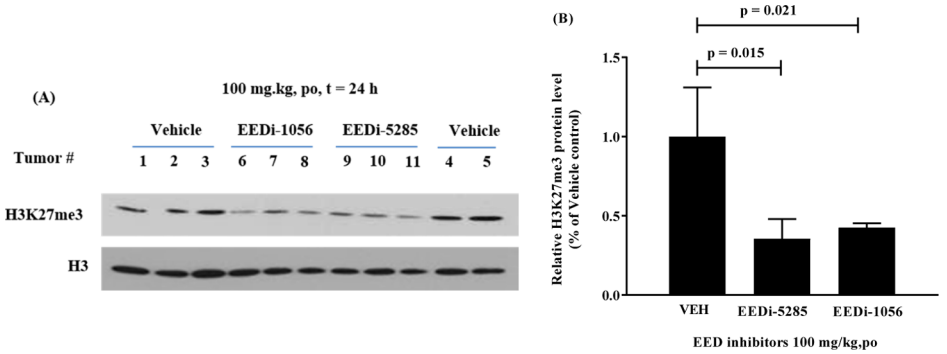

Figure 4. Pharmacodynamic analysis of EEDi-5285 and EEDi-1056 in KARPAS422 xenograft tumors. SCID mice bearing KARPAS422 tumors were treated with a single oral administration of EEDi-5285 or EEDi-1056 at 100 mg/kg. Mice were euthanized at the 24 h time-point and tumor tissues were collected. Histone proteins were extracted from the treated cells with the EpiQuik Total Histone Extraction Kit, and the level of H3K27me3 was examined by Western blotting analysis. Total histone H3 was used as the loading control. Three mice were used for each compound with each mouse bearing one tumor.

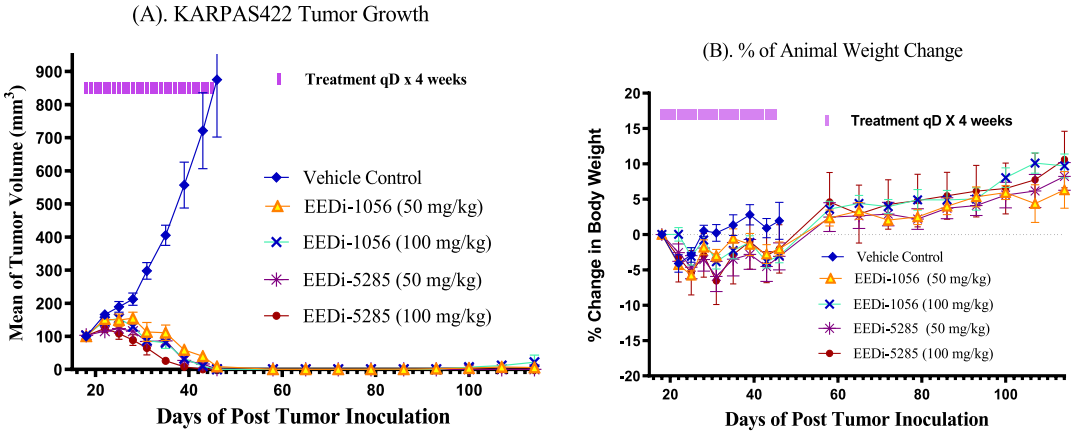

Figure 5. (A) Antitumor activity of EEDi-5285 and EEDi-1056 in a KARPAS422 xenograft model in SCID mice. Each group had seven mice and each mouse had one tumor. (B) Changes in animal body weights.

of the synthesis of the compounds in Table 2 are provided in the Supporting Information.

In Scheme 2, the bicyclic compound **54** was made from the corresponding amine **52** using formylation followed by cyclization using $POCl_3$. Upon Cu-mediated trifluoromethylation[21] and sulfonation,[22] intermediate **58** afforded the corresponding compounds **20** and **21**, respectively. Intermediate **58** upon Pd-catalyzed P-arylation[23] with dialkyl phosphine oxide formed compound **22** (Scheme 2).

CONCLUSIONS

Starting from a previously reported EED inhibitor (**7**), we performed structure-guided design and optimization to identify potent and efficacious new EED inhibitors. Our efforts have yielded exceptionally potent EED inhibitors. A number of these new EED inhibitors bind to EED with subnanomolar IC_{50} values and inhibit cell growth with subnanomolar to low nanomolar IC_{50} values in the KARPAS422 cell line and low picomolar IC_{50} values in the Pfeiffer cell line. Among these, EEDi-5285 and EEDi-1056 show excellent PK profiles in mice. Both EEDi-5285 and EEDi-1056 are capable of achieving complete and long-lasting tumor regression in the KARPAS422 xenograft model in mice with oral administration and at well-tolerated dose schedules. Determination of cocrystal structures of EEDi-5285 and EEDi-1056 complexed with EED defines their precise structural basis for their high binding affinity.

Previous studies have reported EED226, A-395, and BR-001 as three of the potent and promising EED inhibitors.[8,9,18] In direct comparison, EEDi-5285 is approximately 100 times more potent than EED226 in binding to EED (0.2 nM vs 17.6 nM) and is >300 times more potent than EED226 in inhibition of cell growth in the KARPAS422 cell line (0.5 nM vs 182

https://dx.doi.org/10.1021/acs.jmedchem.0c00479
J. Med. Chem. 2020, 63, 7252−7267

Scheme 1. Synthesis of Compounds 8−19[a]

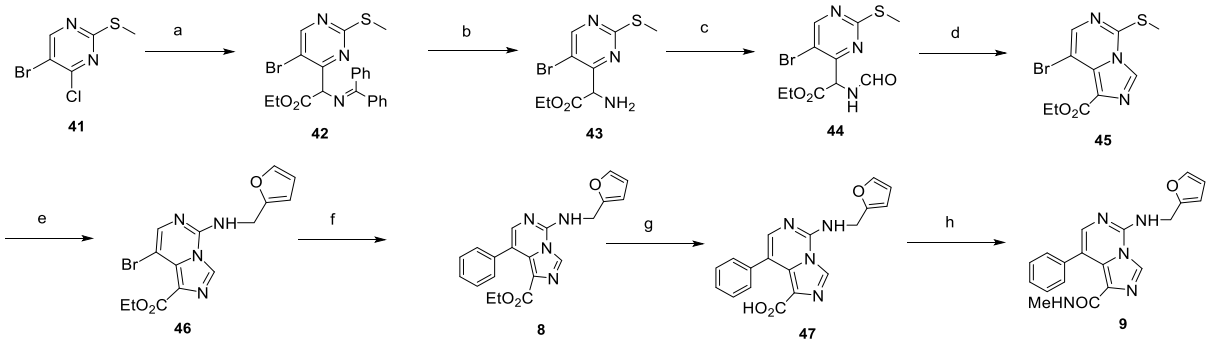

[a]Reagents and conditions: (a) ethyl 2-(diphenylmethyleneamino)acetate, NaH, rt, 2 h; (b) 3 N HCl in THF, rt, 1 h, 70%; (c) HCO_2H, Ac_2O, rt, 2 h; (d) $POCl_3$, dioxane, reflux, 4 h, 70%; (e) (i) mCPBA, DCM, (ii) furan-2-ylmethanamine, rt, 3 h, 55%; (f) phenylboronic acid, $Pd(PPh_3)_4$, K_2CO_3, dioxane−H_2O, 90 °C overnight, 90%; (g) $Li(OH)_2$, THF−H_2O, 90%; (h) $MeNH_2$·HCl, DIPEA, HATU, 90%

Scheme 2. Synthesis of Compounds 7 and 20−34[a]

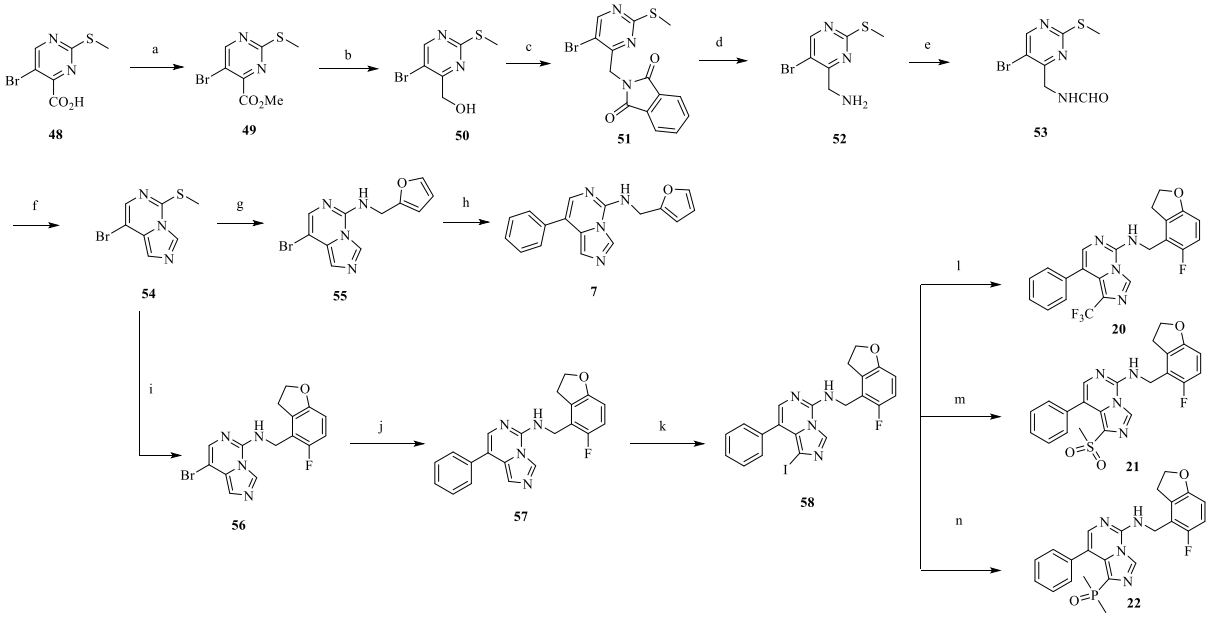

[a]Reagents and conditions: (a) CH_3COCl, MeOH, 79%; (b) DIBAL-H, 56%; (c) DIAD, PPh_3, phthalidomide, 70%; (d) NH_2·NH_2. H_2O, EtOH, 80%; (e) HCO_2H, Ac_2O, 60%; (f) $POCl_3$, dioxane, 47.0%; (g) (i) mCPBA, DCM, (ii) furan-2-ylmethanamine, rt, 3 h, 52%; (h) phenylboronic acid, $Pd(PPh_3)_4$, K_2CO_3, dioxane−H_2O, 90 °C overnight, 88%; (i) (5-fluoro-2,3-dihydrobenzofuran-4-yl)methanamine, 40 °C, 24 h, 60%; (j) phenylboronic acid, $Pd(PPh_3)_4$, K_2CO_3, dioxane−H_2O, 90 °C overnight, 88%; (k) NIS, DMF, 0 °C, 70%; (l) copper (I) iodide, methyl 2,2-difluoro-2-(fluorosulfonyl)acetate, $PdCl_2(dppf)Cl_2$, 42%; (m) $MeSO_2Na$, CuI, DMSO, 50%; (n) dimethylphosphine oxide, $Pd_2(dba)_3$, xantphos, Et_3N, dioxane, 40%.

nM). While EED226 was capable of achieving complete KARPAS422 cell tumor regression at 300 mg/kg with twice daily administration via oral gavage,[8] EEDi-5285 achieved complete and long-lasting tumor regression with daily administration via oral gavage at 50 mg/kg in the same model. A-395 was shown to have an IC_{50} value of 69 nM in the Pfeiffer cell line with a 10-day treatment time and was able to inhibit tumor growth by 84% at 300 mg/kg with twice a week subcutaneous injections for 5 weeks.[9] BR-001 was shown to be 2−3 times more potent than EED226 in cells and capable of inhibiting tumor growth by 85% at 100 mg/kg with twice daily administration.[18] Therefore, EEDi-5285 is the most potent and efficacious EED inhibitor reported to date and warrants extensive preclinical studies.

EXPERIMENTAL SECTION

General Information. Unless otherwise stated, all commercial reagents were used as supplied without further purification, and all reactions were performed under a nitrogen atmosphere in dry solvents under anhydrous conditions. NMR spectra were obtained with a Bruker 400 Ascend spectrometer at a ^1H frequency of 400 MHz and a ^{13}C frequency of 100 MHz. Chemical shifts (δ) are reported in parts per million (ppm) relative to an internal standard. The final products were purified on a preparative high-performance liquid chromatography (HPLC) column (Waters 2545, Quaternary Gradient Module) with a SunFire Prep C18 OBD 5 μm 50 × 100 mm^2 reverse phase column. The mobile phase was a gradient of solvent A (H_2O with 0.1% TFA) and solvent B (CH_3CN with 0.1% of TFA) at a flow rate of 60 mL/min and 1%/min increase of solvent B. All final compounds have purity ≥95% as determined by Waters ACQUITY ultra-performance liquid chromatography (UPLC) using a reverse phase column (SunFire, C18, 5 μm, 4.6 × 150 mm^2) and a solvent gradient

https://dx.doi.org/10.1021/acs.jmedchem.0c00479
J. Med. Chem. 2020, 63, 7252−7267

Scheme 3. Synthesis of Compounds 35−40[a]

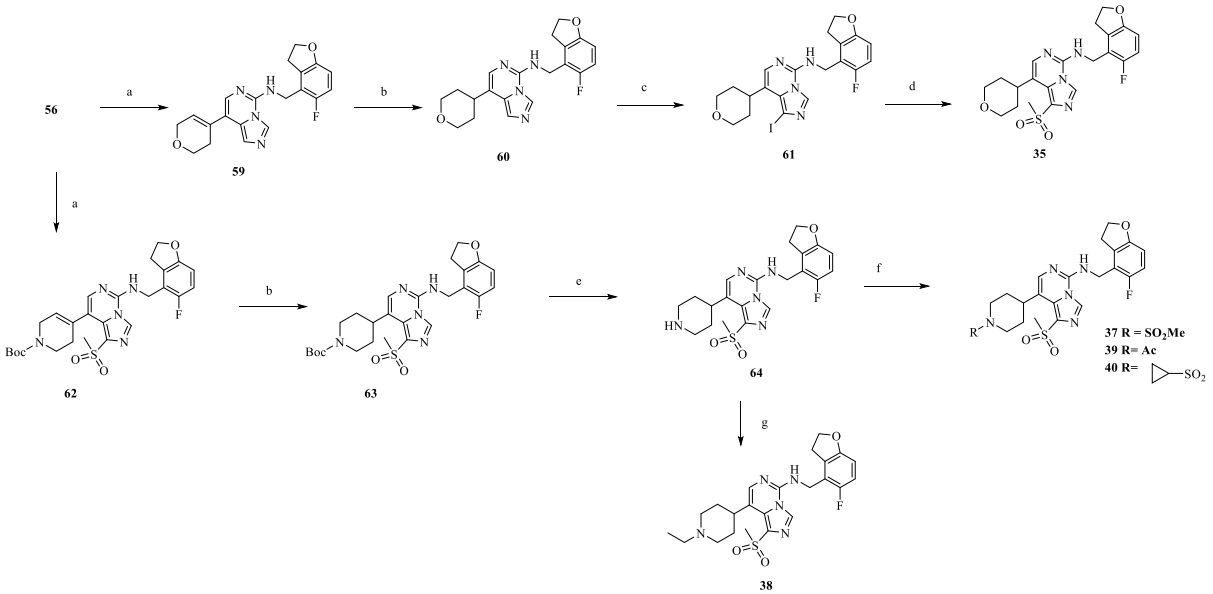

[a]Reagents and conditions: (a) boronic acid, $Pd(PPh_3)_4$, K_2CO_3, dioxane−H_2O, 90 °C overnight, 88%; (b) H_2, Pd/C, MeOH; (c) NIS, DMF, 0 °C, 70%; (d) $MeSO_2Na$, CuI, DMSO, 50%; (e) TFA, DCM; (f) DCM, Et_3N, alkyl chloride; (g) DCM/AcOH (1:1), alkyl aldehyde or ketone, $NaBH(OAc)_3$.

Scheme 4. Synthesis of (5-Fluoro-2,3-dihydrobenzofuran-4-yl)methanamine[a]

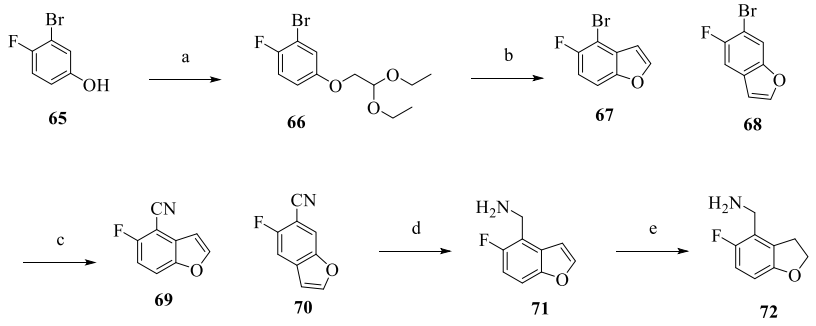

[a]Reagents and conditions: (a) 2-bromo-1,1-diethoxyethane, K_2CO_3, DMF, 110 °C; (b) PPA, toluene, 90 °C; (c) $Zn(CN)_2$, $Pd(PPh_3)_4$, DMF; (d) LAH, THF, 50 °C; (e) H_2, Pd/C, 50 °C.

of A (H_2O with 0.1% of TFA) and solvent B (CH_3CN with 0.1% of TFA). Electrospray ionization (ESI) mass spectrometry (MS) analysis was performed on a Thermo Scientific LCQ Fleet mass spectrometer.

*Ethyl 2-(5-Bromo-2-(methylthio)pyrimidin-4-yl)-2-((diphenylmethylene)amino)acetate (**42**).* A solution of ethyl 2-(diphenylmethyleneamino)acetate (18.4 g, 69 mmol) in DMSO (50 mL) was added dropwise at 0 °C to a suspension of 60% NaH (5.0 g, 125.5 mmol) in anhydrous DMSO (70 mL). The reaction mixture turned orange immediately. After 5 min, 5-bromo-4-chloro-2-(methylthio)pyrimidine (**41**, 15 g, 62.7 mmol) in 50 mL of DMSO was added dropwise. The mixture was then stirred at rt for 2 h. Then, the reaction mixture was quenched by careful addition of aq NH_4Cl solution. The mixture was extracted with EtOAc, washed with brine, dried, and concentrated and used as obtained in the next step. LC−MS: $[M + H]^+$, 470.01.

*Ethyl 2-Amino-2-(5-bromo-2-(methylthio)pyrimidin-4-yl)acetate (**43**).* 3 N HCl in H_2O (10 mL) was added at 0 °C to a solution of crude compound **42** (5.0 g, 10.6 mmol) in THF (50 mL). The mixture was stirred at rt for 1 h and the reaction mixture was then concentrated followed by adjustment to pH 8−9 with aq Na_2CO_3 solution. The mixture was extracted with DCM and washed with brine. Concentration under reduced pressure followed by purification by flash chromatography (0−100% EtOAc/hexane) gave the desired compound **43** (2.26 g) in 70% overall yield. ^1H NMR (400 MHz, $CDCl_3$): δ 8.58 (s, 1H), 4.99 (s, 1H), 4.26−4.16 (m, 2H), 2.53 (s, 3H), 1.26 (t, 3H). LC−MS: $[M + H]^+$, 305.95.

*Ethyl 2-(5-Bromo-2-(methylthio)pyrimidin-4-yl)-2-formamidoacetate (**44**).* A mixture of HCO_2H (4 mL) and Ac_2O (4 mL) was heated at 50 °C for 1 h. The reaction mixture was cooled to rt and added to a solution of compound **43** (2.0 g, 6.55 mmol) in DCM (20 mL). The mixture was stirred at rt for 2 h. After completion of the reaction, the mixture was concentrated. The mixture was extracted with DCM (2 × 50 mL) and washed successively with H_2O (20 mL) and brine (10 mL). The organic phase was dried over Na_2SO_4, filtered, and concentrated to afford the crude title compound **44** as an oil, which was used in the next steps without further purification. ^1H NMR (400 MHz, $CDCl_3$): δ 8.63 (s, 1H), 8.32 (s, 1H), 7.02 (br s, 1H), 6.20 (d, 1H), 4.31−4.11 (m, 2H), 2.54 (s, 3H), 1.27 (t, 3H). LC−MS: $[M + H]^+$, 334.05.

*Ethyl 8-Bromo-5-(methylthio)imidazo[1,5-c]pyrimidine-1-carboxylate (**45**).* $POCl_3$ (1.5 mL) was added dropwise to a solution of compound **44** (2.0 g, crude) in dioxane (20 mL). The reaction mixture was heated under reflux for 4 h. The mixture was cooled to rt and concentrated. Ice/H_2O (50 mL) was added, and the mixture was adjusted to pH 8 with satd. aq $NaHCO_3$. The mixture was extracted with DCM (2 × 50 mL), washed with brine (10 mL), dried over

https://dx.doi.org/10.1021/acs.jmedchem.0c00479
J. Med. Chem. 2020, 63, 7252−7267

Na_2SO_4, and filtered. The filtrate was concentrated, and the residue was purified by silica gel column chromatography (eluting with 50−100% EtOAc/hexane) to afford the title compound **45** as a white solid (1.42 g, 4.59 mmol) in 70% overall yield over two steps. ^{1}H NMR (400 MHz, DMSO-d_6): 8.67 (s, 1H), 7.99 (s, 1H), 4.33 (q, 2H), 2.76 (s, 3H), 1.34 (t, 3H). LC−MS: $[M + H]^+$, 315.70.

*Ethyl 8-Bromo-5-((furan-2-ylmethyl)amino)imidazo[1,5-c]pyrimidine-1-carboxylate (**46**).* *m*-CPBA (464 mg, 2.7 mmol, ≤77%, 1.5 equiv) was added at 0 °C to a solution of compound **45** (567 mg, 1.8 mmol, 1.0 equiv) in DCM (18 mL). After 45 min, Et_3N (1 mL, 7.6 mmol, 4 equiv) was added at 0 °C and stirred for 2 min, followed by addition of furan-2-ylmethanamine (175 mg, 1.8 mmol). The reaction mixture was then stirred at rt for 3 h. Then, the reaction mixture was concentrated and the residue was purified by silica gel column chromatography (eluting with 50−100% EtOAc/hexane) to afford the title compound **46** (361 mg, 0.99 mmol) in 55% yield. ^{1}H NMR (400 MHz, MeOH-d_4): δ 8.58 (s, 1H), 7.70 (d, J = 2.1 Hz, 1H), 7.47 (dd, J = 1.8, 1.0 Hz, 1H), 6.39 (dt, J = 3.2, 1.1 Hz, 2H), 4.78 (t, J = 0.9 Hz, 2H), 4.46−4.36 (m, 2H), 1.43−1.35 (m, 3H). LC−MS: $[M + H]^+$, 365.01.

*Ethyl 5-((Furan-2-ylmethyl)amino)-8-phenylimidazo[1,5-c]pyrimidine-1-carboxylate (**8**).* Potassium carbonate (227 mg, 1.64 mmol), phenylboronic acid (168 mg, 0.82 mmol), and $Pd(PPh_3)_4$ (63 mg, 0.055 mmol) were added to a solution of compound **46** (200 mg, 0.55 mmol) in a mixed solvent (dioxane/H_2O = 10:2.5 mL). The resulting mixture was stirred under N_2 at 90 °C overnight. The mixture was then cooled to rt, and the solvent was removed in vacuo. The residue was purified with silica gel chromatography (eluted with 0−10% MeOH/DCM) to afford title compound **8** (159 mg, 0.34 mmol) in 80% yield. ^{1}H NMR (400 MHz, $CDCl_3$): δ 8.81 (s, 1H), 7.49 (d, J = 1.0 Hz, 1H), 7.41 (d, J = 6.7 Hz, 3H), 7.34 (dq, J = 3.3, 1.7 Hz, 3H), 6.35 (d, J = 3.2 Hz, 1H), 6.30 (dt, J = 3.1, 1.4 Hz, 1H), 4.87 (s, 2H), 3.87 (q, J = 7.1 Hz, 2H), 0.88 (t, J = 7.1 Hz, 3H). LC−MS: $[M + H]^+$, 363.01.

*5-((Furan-2-ylmethyl)amino)-8-phenylimidazo[1,5-c]pyrimidine-1-carboxylic Acid (**47**).* A mixture of **8** (40 mg, 0.11 mmol, 1 equiv) and LiOH (26 mg, 1.10 mmol, 10 equiv) in THF (4 mL) and H_2O (2.0 mL) was heated at 70 °C overnight. 3 N aq HCl was added dropwise at 0 °C to pH 2−3. The mixture was concentrated, and the residue was purified by HPLC to afford the title compound **47** (33 mg, 0.099 mmol) in 90% yield. LC−MS: $[M + H]^+$, 335.10.

*N-(Furan-2-ylmethyl)-1-(((methylamino)oxy)carbonyl)-8-phenylimidazo[1,5-c]pyrimidin-5-amine (**9**).* Methylamine hydrochloride (4 mg, 0.058 mmol) and diisopropylethylamine (50 μL, 0.29 mmol) were added to a solution of compound **47** (10 mg, 0.029 mmol) in DMF (1 mL). The reaction mixture was stirred at rt for 10 min and then HATU (11 mg, 0.029 mmol) was added. The reaction mixture was allowed to warm to rt and stirred at rt overnight. The mixture was concentrated, and the residue was purified by HPLC to afford the title compound **9**(9 mg, 0.026 mmol) in 90% yield. ^{1}H NMR (400 MHz, $CDCl_3$): δ 9.22 (s, 1H), 7.55−7.43 (m, 3H), 7.38−7.30 (m, 3H), 6.40 (s, 1H), 6.36 (s, 1H), 6.31 (br s, 1H), 4.86 (s, 2H), 2.54 (s, 3H). LC−MS: $[M + H]^+$, 348.13.

*Ethyl 5-(Benzylamino)-8-phenylimidazo[1,5-c]pyrimidine-1-carboxylate (**10**).* ^{1}H NMR (400 MHz, DMSO-d_6): δ 8.80 (d, J = 5.9 Hz, 1H), 8.78 (s, 1H), 7.49−7.22 (m, 11H), 4.80 (d, J = 5.5 Hz, 2H), 3.68 (q, J = 7.1 Hz, 2H), 0.74 (t, J = 7.1 Hz, 3H). LC−MS: $[M + H]^+$, 373.16.

*Ethyl 5-((2-Methoxybenzyl)amino)-8-phenylimidazo[1,5-c]pyrimidine-1-carboxylate (**11**).* ^{1}H NMR (400 MHz, MeOH-d_4): δ 8.71 (s, 1H), 7.46−7.33 (m, 7H), 7.33−7.26 (m, 1H), 7.03 (dd, J = 8.3, 1.1 Hz, 1H), 6.94 (td, J = 7.5, 1.1 Hz, 1H), 4.84 (s, 2H), 3.91 (s, 3H), 3.80 (q, J = 7.2 Hz, 2H), 0.86 (t, J = 7.1 Hz, 3H). LC−MS: $[M + H]^+$, 403.16.

*Ethyl 5-((2-Fluoro-6-methoxybenzyl)amino)-8-phenylimidazo[1,5-c]pyrimidine-1-carboxylate (**12**).* ^{1}H NMR (400 MHz, MeOH-d_4): δ 8.70 (s, 1H), 7.48−7.31 (m, 7H), 6.90 (dt, J = 8.4, 0.9 Hz, 1H), 6.80 (ddd, J = 9.3, 8.4, 0.9 Hz, 1H), 4.88 (s, 2H), 3.91 (s, 3H), 3.79 (q, J = 7.1 Hz, 2H), 0.86 (t, J = 7.1 Hz, 3H). LC−MS: $[M + H]^+$, 421.16.

*Ethyl 5-((2-Fluoro-5-methoxybenzyl)amino)-8-phenylimidazo[1,5-c]pyrimidine-1-carboxylate (**13**).* ^{1}H NMR (400 MHz, MeOH-d_4): δ 8.70 (s, 1H), 7.50−7.29 (m, 6H), 7.15−6.98 (m, 2H), 6.91−6.77 (m, 1H), 4.86 (s, 2H), 3.85−3.77 (m, 2H), 3.76 (s, 3H), 0.86 (t, J = 7.1 Hz, 3H). LC−MS: $[M + H]^+$, 421.15.

*Ethyl 5-((2-Fluoro-4-methoxybenzyl)amino)-8-phenylimidazo[1,5-c]pyrimidine-1-carboxylate (**14**).* ^{1}H NMR (400 MHz, DMSO-d_6): δ 8.78 (s, 1H), 8.69 (s, 1H), 7.51−7.25 (m, 7H), 6.86 (dd, J = 12.2, 2.5 Hz, 1H), 6.77 (dd, J = 8.5, 2.5 Hz, 1H), 4.74 (s, 2H), 3.85−3.77 (m, 2H), 3.76 (s, 3H), 0.74 (t, J = 7.1 Hz, 3H). LC−MS: $[M + H]^+$, 421.15.

*Ethyl 5-((Benzo[d][1,3]dioxol-4-ylmethyl)amino)-8-phenylimidazo[1,5-c]pyrimidine-1-carboxylate (**15**).* ^{1}H NMR (400 MHz, MeOH-d_4): δ 8.70 (s, 1H), 7.47−7.31 (m, 6H), 6.95 (ddt, J = 7.7, 1.4, 0.7 Hz, 1H), 6.88−6.75 (m, 2H), 5.99 (s, 2H), 4.84 (s, 2H), 3.80 (q, J = 7.1 Hz, 2H), 0.86 (t, J = 7.1 Hz, 3H). LC−MS: $[M + H]^+$, 417.14.

*Ethyl 5-(((2,3-Dihydrobenzofuran-7-yl)methyl)amino)-8-phenylimidazo[1,5-c]pyrimidine-1-carboxylate (**16**).* ^{1}H NMR (400 MHz, DMSO-d_6): δ 8.80 (s, 1H), 8.66 (t, J = 5.5 Hz, 1H), 7.44−7.26 (m, 6H), 7.15 (t, J = 8.5 Hz, 2H), 6.80 (t, J = 7.5 Hz, 1H), 4.70 (d, J = 5.4 Hz, 2H), 4.59 (t, J = 8.8 Hz, 2H), 3.68 (q, J = 7.1 Hz, 2H), 3.21 (t, J = 8.7 Hz, 2H), 0.74 (t, J = 7.1 Hz, 3H). LC−MS: $[M + H]^+$, 415.17.

*Ethyl 5-(((2,3-Dihydrobenzofuran-4-yl)methyl)amino)-8-phenylimidazo[1,5-c]pyrimidine-1-carboxylate (**17**).* ^{1}H NMR (400 MHz, DMSO-d_6): δ 8.80 (s, 1H), 8.70 (t, J = 5.5 Hz, 1H), 7.48−7.25 (m, 6H), 7.07 (t, J = 7.8 Hz, 1H), 6.87 (d, J = 7.7 Hz, 1H), 6.69 (d, J = 7.8 Hz, 1H), 4.72 (d, J = 5.3 Hz, 2H), 4.55 (t, J = 8.7 Hz, 2H), 3.68 (q, J = 7.1 Hz, 2H), 3.25 (t, J = 8.7 Hz, 2H), 0.74 (t, J = 7.1 Hz, 3H). LC−MS: $[M + H]^+$, 415.17.

*Ethyl 5-(((5-Fluoro-2,3-dihydrobenzofuran-4-yl)methyl)amino)-8-phenylimidazo[1,5-c]pyrimidine-1-carboxylate (**18**).* ^{1}H NMR (400 MHz, MeOH-d_4): δ 8.70 (s, 1H), 7.50−7.25 (m, 6H), 6.91−6.83 (m, 1H), 6.67 (dd, J = 8.6, 3.9 Hz, 1H), 4.84 (d, J = 1.1 Hz, 2H), 4.59 (t, J = 8.7 Hz, 2H), 3.80 (q, J = 7.2 Hz, 2H), 3.44−3.35 (m, 2H), 0.86 (t, J = 7.1 Hz, 3H). LC−MS: $[M + H]^+$, 433.15.

*5-(((5-Fluoro-2,3-dihydrobenzofuran-4-yl)methyl)amino)-N-methyl-8-phenylimidazo[1,5-c]pyrimidine-1-carboxamide (**19**).* ^{1}H NMR (400 MHz, MeOH-d_4): δ 8.64 (s, 1H), 7.50−7.29 (m, 6H), 6.92−6.81 (m, 1H), 6.67 (dd, J = 8.7, 3.9 Hz, 1H), 4.83 (d, J = 1.2 Hz, 2H), 4.59 (t, J = 8.7 Hz, 2H), 3.38 (t, J = 8.7 Hz, 2H), 2.51 (s, 3H). LC−MS: $[M + H]^+$, 418.16.

*Methyl 5-Bromo-2-(methylthio)pyrimidine-4-carboxylate (**49**).* Acetyl chloride (3.1 mL, 43.8 mmol) was added dropwise to MeOH (50 mL) at 0−5 °C. The resulting mixture was stirred at this temperature for 5 min; then, 5-bromo-2-(methylthio)pyrimidine-4-carboxylic acid (5.5 g, 22.2 mmol) was added. The reaction mixture was heated to reflux for 1 h and then cooled to rt. The reaction mixture was poured into satd. aq. $NaHCO_3$ solution (100 mL). The mixture was extracted with DCM (3 × 100 mL), washed with H_2O (50 mL), dried (Na_2SO_4), filtered, and concentrated, and the residue was recrystallized from petroleum ether to give the title compound **49** as a yellow solid (4.6 g, 34.6 mmol) in 79% yield. ^{1}H NMR (400 MHz, $CDCl_3$): δ 8.71 (s, 1H), 4.0 (s, 3H), 2.59 (s, 3H). LC−MS: $[M + H]^+$, 263.10.

*(5-Bromo-2-(methylthio)pyrimidin-4-yl)methanol (**50**).* DIBAL-H (4.6 mL, 4.60 mmol, 1 M in cyclohexane) was added dropwise to a solution of methyl 5-bromo-2-(methylthio)pyrimidine-4-carboxylate (**49**, 600 mg, 2.28 mmol) in DCM (15 mL) at −60 °C. The reaction mixture was maintained at −60 to −15 °C for 30 min and then was allowed to rise to rt and stirred for another 12 h. The reaction mixture was cooled to 0 °C and was quenched with satd. aq NH_4Cl (50 mL). The resulting mixture was extracted with DCM (3 × 100 mL), washed with brine (50 mL), dried over Na_2SO_4, filtered, and concentrated. The residue was purified by column chromatography (eluting with 0−50% EtOAc/hexane) to afford the title compound **50** as a yellow solid (300 mg) in 56% yield. ^{1}H NMR (400 MHz, $CDCl_3$): δ 8.52 (s, 1H), 4.72 (d, J = 4.8 Hz, 2H), 3.85 (t, J = 4.9 Hz, 1H), 2.61 (s, 3H). LC−MS: $[M + H]^+$, 235.02.

https://dx.doi.org/10.1021/acs.jmedchem.0c00479
J. Med. Chem. 2020, 63, 7252−7267

*2-((5-Bromo-2-(methylthio)pyrimidin-4-yl)methyl)isoindoline-1,3-dione (**51**).* A solution in THF (10 mL) of (5-bromo-2-(methylthio)pyrimidin-4-yl)methanol (**50**, 1.69 g, 7.22 mmol), phthalimide (1.27 g, 8.66 mmol), and triphenylphosphine (2.19 g, 10.84 mmol) was mixed with DIAD (1.88 g, 10.84 mmol) under cooling with ice and stirred at rt overnight. After completion of the reaction, the mixture was diluted with EtOAc, and the organic layer was washed with saturated brine, dried over Na_2SO_4, and evaporated under reduced pressure. The residue was purified by column chromatography (eluting with 0−50% EtOAc/hexane) to afford the desired product **51** (479 mg) in 70% yield. ^{1}H NMR (400 MHz, $CDCl_3$): δ 8.51 (s, 1H), 7.95 (dd, J = 5.4, 3.1 Hz, 2H), 7.85−7.76 (m, 2H), 5.02 (s, 2H), 2.05 (s, 3H). LC−MS: $[M + H]^+$, 363.12.

*(5-Bromo-2-(methylthio)pyrimidin-4-yl)methanamine (**52**).* Compound **51** (910 mg, 2.51 mmol) in EtOH (10 mL) was stirred with $NH_2NH_2{\cdot}H_2O$ (0.157 mL, 5.02 mmol) at rt for 4 h. After completion of the reaction, the solid was filtered and washed with EtOH, and the filtrate was evaporated under reduced pressure. It was purified by reverse phase chromatography (eluting with 0−20% CH_3CN/H_2O) to afford the title compound **52** as a colorless liquid in 80% yield. ^{1}H NMR (400 MHz, $CDCl_3$): δ 8.49 (s, 1H), 4.02 (s, 2H), 2.59 (s, 3H). LC−MS: $[M + H]^+$, 236.10.

*N-((5-Bromo-2-(methylthio)pyrimidin-4-yl)methyl)formamide (**53**).* A mixture of HCO_2H (4 mL) and Ac_2O (4 mL) was heated at 50 °C for 1 h. The reaction mixture was cooled to rt and added to a solution of compound **52** (1.52 g, 6.55 mmol) in DCM (20 mL). The mixture was stirred at rt for 2 h. After completion of the reaction, the mixture was concentrated, then extracted with DCM (2 × 50 mL) and washed successively with H_2O (20 mL) and brine (10 mL). The organic phase was dried over Na_2SO_4, filtered, and concentrated to afford the crude title compound **53** as an oil, which was used in the next steps without further purification. ^{1}H NMR (400 MHz, $CDCl_3$): δ 8.56 (s, 1H), 8.40 (q, J = 1.2 Hz, 1H), 6.99 (s, 1H), 4.63 (dd, J = 4.6, 1.0 Hz, 2H), 2.59 (s, 3H). LC−MS: $[M + H]^+$, 262.12.

*8-Bromo-5-(methylthio)imidazo[1,5-c]pyrimidine (**54**).* $POCl_3$ (0.43 mL, 4.60 mmol) was added dropwise to a solution of compound **53** (800 mg, 3.06 mmol) in dioxane (30 mL). The reaction mixture was heated under reflux for 2 h. Ice−H_2O (50 mL) was added, and the mixture was adjusted to pH 8 with satd. aq $NaHCO_3$. The mixture was extracted with DCM (4 × 50 mL), washed with brine (30 mL), dried over Na_2SO_4, and filtered. The filtrate was concentrated, and the residue was purified by column chromatography (eluting with 0−50% EtOAc/hexane) to afford the title compound **54** as a yellow solid (350 mg, 47.0%). ^{1}H NMR (400 MHz, $CDCl_3$): δ 8.20 (s, 1H), 7.55 (d, J = 2.0 Hz, 2H), 2.77 (s, 3H). LC−MS: $[M + H]^+$, 244.01.

*8-Bromo-N-(furan-2-ylmethyl)imidazo[1,5-c]pyrimidin-5-amine (**55**).* *m*-CPBA (464 mg, 2.7 mmol, ≤77%, 1.5 equiv) was added at 0 °C to a solution of compound **54** (439 mg, 1.8 mmol, 1.0 equiv) in DCM (18 mL). After 45 min, Et_3N (1 mL, 7.6 mmol, 4 equiv) was added at 0 °C and stirred for 2 min, followed by addition of furan-2-ylmethanamine (175 mg, 1.8 mmol). The reaction mixture was then stirred at rt for 3 h. Then, the reaction mixture was concentrated and the residue was purified by silica gel column chromatography (eluting with 50−100% EtOAc/hexane) to afford the title compound **55** (274 mg, 0.93 mmol) in 52% yield. LC−MS: $[M + H]^+$, 294.12.

*N-(Furan-2-ylmethyl)-8-phenylimidazo[1,5-c]pyrimidin-5-amine (**7**).* Potassium carbonate (227 mg, 1.64 mmol), phenylboronic acid (168 mg, 0.82 mmol), and $Pd(PPh_3)_4$ (63 mg, 0.055 mmol) were added to a solution of compound **55** (160 mg, 0.55 mmol) in a mixed solvent (dioxane/H_2O = 10:2.5 mL). The resulting mixture was stirred under N_2 at 90 °C overnight. The mixture was then cooled to rt, and the solvent was removed in vacuo. The residue was purified with silica gel chromatography (eluting with 0−10% MeOH/DCM) to afford title compound **7** (159 mg, 0.34 mmol) in 80% yield. ^{1}H NMR (400 MHz, $CDCl_3$): δ 10.13 (s, 1H), 7.66 (s, 1H), 7.61 (d, J = 1.0 Hz, 1H), 7.57−7.51 (m, 4H), 7.51−7.45 (m, 1H), 7.37 (dd, J = 1.8, 0.8 Hz, 1H), 6.41 (dd, J = 3.2, 0.8 Hz, 1H), 6.34 (dd, J = 3.2, 1.8 Hz, 1H), 4.89 (s, 2H). LC−MS: $[M + H]^+$, 291.11.

*8-Bromo-N-((5-fluoro-2,3-dihydrobenzofuran-4-yl)methyl)-imidazo[1,5-c]pyrimidin-5-amine (**56**).* A mixture of compound **54** (1.0 g, 4.1 mmol) and (5-fluoro-2,3-dihydrobenzofuran-4-yl)-methanamine (1.41 g, 8.2 mmol) was heated at 40 °C and stirred for 24 h. After cooling to rt, the crude mixture was purified by reverse phase chromatography (eluting with 0−70% CH_3CN/H_2O) to afford the title compound **56** as a yellow solid in 60% yield. ^{1}H NMR (400 MHz, MeOH-d_4): δ 8.58 (s, 1H), 7.38 (s, 1H), 7.32 (s, 1H), 6.91−6.80 (m, 1H), 6.65 (dd, J = 8.7, 3.9 Hz, 1H), 4.74 (s, 2H), 4.62−4.52 (m, 2H), 3.37 (s, 2H). LC−MS: $[M + H]^+$, 363.01.

*N-((5-Fluoro-2,3-dihydrobenzofuran-4-yl)methyl)-8-phenylimidazo[1,5-c]pyrimidin-5-amine (**57**).* Potassium carbonate (227 mg, 1.64 mmol), phenylboronic acid (168 mg, 0.82 mmol), and $Pd(PPh_3)_4$ (63 mg, 0.055 mmol) were added to a solution of compound **56** (200 mg, 0.55 mmol) in a mixed solvent (dioxane/H_2O = 10:2.5 mL). The resulting mixture was stirred under N_2 at 90 °C overnight. The mixture was then cooled to rt, and the solvent was removed in vacuo. The residue was purified with silica gel chromatography (eluting with 0−10% MeOH/DCM) to afford title compound **57** (174 mg, 0.34 mmol) in 88% yield. LC−MS: $[M + H]^+$, 361.13.

*N-((5-Fluoro-2,3-dihydrobenzofuran-4-yl)methyl)-1-iodo-8-phenylimidazo[1,5-c]pyrimidin-5-amine (**58**).* NIS (278 mg, 1.24 mmol) was added to a solution of compound **57** (500 mg, 1.38 mmol) in DMF (10 mL) at 0 °C and stirred at rt for 15 min. The mixture was extracted with DCM (4 × 50 mL), washed with brine (30 mL), dried (Na_2SO_4), and filtered. The filtrate was concentrated, and the residue was purified by column chromatography (eluting with 20−50% EtOAc/hexane) to afford the title compound **58** as a yellow solid (610 mg, 1.26 mmol, 70%). LC−MS: $[M + H]^+$, 487.03.

*N-((5-Fluoro-2,3-dihydrobenzofuran-4-yl)methyl)-8-phenyl-1-(trifluoromethyl)-imidazo[1,5-c]pyrimidin-5-amine (**20**).* A solution of compound **58** (50 mg, 0.1 mmol) in DMF (5 mL) was added to a mixture of cuprous iodide (190 mg, 1.0 mmol), methyl 2,2-difluoro-2-(fluorosulfonyl)acetate (192 mg, 1.0 mmol), and $PdCl_2(dppf)Cl_2$ (7 mg, 0.01 mmol). The reaction was stirred at 90 °C overnight, then cooled down to rt, and quenched by being poured into H_2O. The mixture was filtered and the filtrate was extracted with Et_2O. The ethereal extract was concentrated, and the residue was purified by HPLC to afford the title compound **20** (16 mg, 0.04 mmol) in 42% yield. ^{1}H NMR (400 MHz, DMSO-d_6): δ 8.85 (s, 1H), 8.61 (s, 1H), 7.44−7.31 (m, 6H), 6.94 (t, J = 8.8 Hz, 1H), 6.71 (dd, J = 8.4, 4.0 Hz, 1H), 4.73 (d, 2H), 4.54 (t, J = 8.8 Hz, 2H), 3.31 (t, J = 8.8 Hz, 2H). LC−MS: $[M + H]^+$, 429.12.

*N-((5-Fluoro-2,3-dihydrobenzofuran-4-yl)methyl)-1-(methylsulfonyl)-8-phenylimidazo[1,5-c]pyrimidin-5-amine (**21**).* A mixture of compound **58** (50 mg, 0.1 mmol), $MeSO_2Na$ (30 mg. 0.3 mmol), and CuI (57 mg. 0.3 mmol) in DMSO (2 mL) was bubbled with N_2 for 5 min, the tube was sealed, and then heated in a microwave reactor at 120 °C for 20 min and then at 100 °C for 3 h. The mixture was concentrated, and the residue was purified by HPLC to afford the title compound **21** (21 mg, 0.05 mmol) in 50% yield. ^{1}H NMR (400 MHz, $CDCl_3$): δ 8.60 (s, 1H), 7.55−7.35 (m, 6H), 6.77 (dd, J = 10.1, 8.7 Hz, 1H), 6.61 (dd, J = 8.7, 3.9 Hz, 1H), 4.82 (s, 2H), 4.61 (t, J = 8.7 Hz, 2H), 3.40 (t, J = 8.7 Hz, 2H), 2.86 (s, 3H). LC−MS: $[M + H]^+$, 439.12.

*(5-(((5-Fluoro-2,3-dihydrobenzofuran-4-yl)methyl)amino)-8-phenylimidazo[1,5-c]pyrimidin-1-yl)dimethylphosphine Oxide (**22**).* Dimethylphosphine oxide (22 mg, 0.3 mmol), $Pd_2(dba)_3$ (9 mg, 0.01 mmol), xantphos (6 mg, 0.01 mmol), and Et_3N (0.2 mL) were added to a solution of compound **58** (50 mg, 0.1 mmol) in dioxane (2 mL). The mixture was purged with argon and heated at 100 °C overnight. The mixture was concentrated, and the residue was purified by HPLC to afford the title compound **22** (17 mg, 0.04 mmol) in 40% yield. ^{1}H NMR (400 MHz, DMSO-d_6): δ 8.85 (s, 1H), 8.52 (s, 1H), 7.58−7.56 (m, 2H), 7.42−7.41 (m, 2H), 7.29 (s, 1H), 6.94 (t, J = 9.2 Hz, 1H), 6.70 (dd, J = 8.4, 4.0 Hz, 1H), 4.73 (d, J = 4.0 Hz, 2H), 4.54 (t, J = 8.8 Hz, 2H), 3.31 (t, J = 8.8 Hz, 2H), 1.21 (s, 1H), 1.18 (s, 1H). LC−MS: $[M + H]^+$, 437.14.

N-((5-Fluoro-2,3-dihydrobenzofuran-4-yl)methyl)-1-(methylsulfonyl)-8-(4(methyl-sulfonyl)phenyl)imidazo[1,5-c]pyrimidin-5-

https://dx.doi.org/10.1021/acs.jmedchem.0c00479
J. Med. Chem. 2020, 63, 7252−7267

*amine (**23**).* ^{1}H NMR (400 MHz, $CDCl_3$): δ 8.12 (s, 1H), 8.03 (d, J = 8.4 Hz, 2H), 7.68 (d, J = 8.4 Hz, 2H), 7.49 (s, 1H), 6.95−6.83 (m, 1H), 6.72 (dd, J = 8.7, 4.0 Hz, 1H), 5.68 (s, 1H), 4.88 (d, J = 4.9 Hz, 2H), 4.66 (t, J = 8.7 Hz, 2H), 3.45 (t, J = 8.7 Hz, 2H), 3.16 (s, 3H), 3.14 (s, 3H). LC−MS: $[M + H]^+$, 517.09.

*N-((5-Fluoro-2,3-dihydrobenzofuran-4-yl)methyl)-8-(4-fluorophenyl)-1(methylsulfonyl)imidazo[1,5-c]pyrimidin-5-amine (**24**).* ^{1}H NMR (400 MHz, MeOH-d_4): δ 8.68 (s, 1H), 7.52−7.31 (m, 3H), 7.18−7.04 (m, 2H), 6.92−6.81 (m, 1H), 6.66 (dd, J = 8.6, 3.8 Hz, 1H), 4.84 (d, J = 1.0 Hz, 2H), 4.59 (t, J = 8.7 Hz, 2H), 3.39 (t, J = 8.7 Hz, 2H), 3.00 (s, 3H). LC−MS: $[M + H]^+$, 457.10.

*N-((5-Fluoro-2,3-dihydrobenzofuran-4-yl)methyl)-8-(2-methyl-4-(methylsulfonyl)phenyl)-1-(methylsulfonyl)imidazo[1,5-c]-pyrimidin-5-amine (**25**).* ^{1}H NMR (400 MHz, DMSO-d_6): δ 8.92 (s, 1H), 8.73 (s, 1H), 7.80 (d, J = 1.9 Hz, 1H), 7.73 (dd, J = 7.9, 2.0 Hz, 1H), 7.45 (d, J = 7.9 Hz, 1H), 7.36 (s, 1H), 6.96 (dd, J = 10.3, 8.6 Hz, 1H), 6.72 (dd, J = 8.6, 3.9 Hz, 1H), 4.75 (q, J = 14.4 Hz, 2H), 4.56 (t, J = 8.7 Hz, 2H), 3.41−3.29 (m, 2H), 3.23 (s, 3H), 2.99 (s, 3H), 2.20 (s, 3H). LC−MS: $[M + H]^+$, 531.10.

*N-((5-Fluoro-2,3-dihydrobenzofuran-4-yl)methyl)-8-(2-methylpyridin-3-yl)-1-(methylsulfonyl)imidazo[1,5-c]pyrimidin-5-amine (**26**).* ^{1}H NMR (400 MHz, MeOH-d_4): δ 8.78 (d, J = 1.5 Hz, 1H), 8.73 (dd, J = 5.9, 1.8 Hz, 1H), 8.44 (dt, J = 7.9, 1.5 Hz, 1H), 7.95 (dd, J = 7.8, 6.0 Hz, 1H), 7.59 (d, J = 0.9 Hz, 1H), 6.88 (td, J = 9.5, 9.1, 1.9 Hz, 1H), 6.67 (dd, J = 8.6, 4.0 Hz, 1H), 4.88 (d, J = 4.9 Hz, 2H), 4.60 (td, J = 8.7, 1.5 Hz, 2H), 3.43 (t, J = 8.7 Hz, 2H), 3.11−3.00 (m, 3H), 2.63 (s, 3H). LC−MS: $[M + H]^+$, 454.12.

*N-((5-Fluoro-2,3-dihydrobenzofuran-4-yl)methyl)-8-(6-methylpyridin-3-yl)-1-(methylsulfonyl)imidazo[1,5-c]pyrimidin-5-amine (**27**).* ^{1}H NMR (400 MHz, MeOH-d_4): δ 8.87−8.80 (m, 1H), 8.76 (d, J = 0.9 Hz, 1H), 8.51 (dd, J = 8.3, 2.1 Hz, 1H), 7.95 (d, J = 8.3 Hz, 1H), 7.62 (d, J = 0.8 Hz, 1H), 6.91−6.82 (m, 1H), 6.66 (dt, J = 9.0, 3.4 Hz, 1H), 4.85 (s, 2H), 4.60 (td, J = 8.7, 1.4 Hz, 2H), 3.41 (t, J = 8.7 Hz, 2H), 3.18 (s, 3H), 2.86 (s, 3H). LC−MS: $[M + H]^+$, 454.12.

*8-(6-Cyclopropylpyridin-3-yl)-N-((5-fluoro-2,3-dihydrobenzofuran-4-yl)methyl)-1-(methylsulfonyl)imidazo[1,5-c]pyrimidin-5-amine (**28**).* ^{1}H NMR (400 MHz, DMSO-d_6): δ 8.92 (s, 1H), 8.86 (s, 1H), 8.58 (s, 1H), 8.01 (s, 1H), 7.48 (d, J = 11.0 Hz, 2H), 6.96 (dd, J = 10.3, 8.7 Hz, 1H), 6.72 (dd, J = 8.7, 3.9 Hz, 1H), 4.75 (d, J = 4.6 Hz, 2H), 4.56 (t, J = 8.7 Hz, 2H), 3.32 (t, J = 8.7 Hz, 2H), 3.11 (s, 3H), 2.26 (dd, J = 9.1, 4.6 Hz, 1H), 1.25−1.11 (m, 2H), 1.07 (t, J = 3.6 Hz, 2H). ^{13}C NMR (100 MHz, DMSO-d_6): δ 159.7, 156.9, 156.2, 154.5, 143.5, 141.9, 130.4, 130.3, 129.7, 126.8, 121.9, 121.8, 121.3, 114.5, 114.3, 108.9, 108.8, 72.0, 43.9, 37.9, 37.8, 29.0, 15.6, 11.5. LC−MS: $[M + H]^+$, 480.14.

*8-(6-(Difluoromethyl)pyridin-3-yl)-N-((5-fluoro-2,3-dihydrobenzofuran-4-yl)methyl)-1-(methylsulfonyl)imidazo[1,5-c]pyrimidin-5-amine (**29**).* ^{1}H NMR (400 MHz, MeOH-d_4): δ 8.74 (s, 1H), 8.73−8.67 (m, 1H), 8.06 (d, J = 2.2 Hz, 1H), 7.77 (d, J = 8.0 Hz, 1H), 7.54 (s, 1H), 6.96−6.77 (m, 2H), 6.73−6.61 (m, 1H), 4.86 (d, J = 1.1 Hz, 2H), 4.60 (t, J = 8.7 Hz, 2H), 3.41 (t, J = 8.7 Hz, 2H), 3.11 (s, 3H). LC−MS: $[M + H]^+$, 490.10.

*N-((5-Fluoro-2,3-dihydrobenzofuran-4-yl)methyl)-1-(methylsulfonyl)-8-(6-(trifluoromethyl)pyridin-3-yl)imidazo[1,5-c]pyrimidin-5-amine (**30**).* ^{1}H NMR (400 MHz, $CDCl_3$): δ 8.74 (d, J = 2.1 Hz, 1H), 8.39 (s, 1H), 8.05−7.91 (m, 1H), 7.78 (dd, J = 8.1, 0.7 Hz, 1H), 7.49 (s, 1H), 6.89−6.72 (m, 1H), 6.65 (dd, J = 8.7, 3.9 Hz, 1H), 6.46 (s, 1H), 4.85 (s, 2H), 4.63 (t, J = 8.7 Hz, 2H), 3.41 (t, J = 8.7 Hz, 2H), 3.08 (s, 3H). LC−MS: $[M + H]^+$, 508.09.

*N-((5-Fluoro-2,3-dihydrobenzofuran-4-yl)methyl)-1-(methylsulfonyl)-8-(6-(methylsulfonyl)pyridin-3-yl)imidazo[1,5-c]pyrimidin-5-amine (**31**).* ^{1}H NMR (400 MHz, MeOH-d_4): δ 8.79 (dd, J = 2.0, 1.0 Hz, 1H), 8.75 (s, 1H), 8.23−8.01 (m, 2H), 7.57 (s, 1H), 6.93−6.80 (m, 1H), 6.67 (dd, J = 8.6, 3.9 Hz, 1H), 4.84 (d, J = 1.0 Hz, 2H), 4.60 (t, J = 8.7 Hz, 2H), 3.41 (t, J = 8.8 Hz, 2H), 3.28 (s, 3H), 3.14 (s, 3H). LC−MS: $[M + H]^+$, 518.08.

*8-(2,6-Dimethylpyridin-3-yl)-N-((5-fluoro-2,3-dihydrobenzofuran-4-yl)methyl)-1-(methylsulfonyl)imidazo[1,5-c]pyrimidin-5-amine (**32**).* ^{1}H NMR (400 MHz, MeOH-d_4): δ 8.54 (s, 1H), 8.05 (d, J = 8.0 Hz, 1H), 7.53 (d, J = 8.0 Hz, 1H), 7.33 (s, 1H), 6.65 (t, J = 9.2 Hz, 1H), 6.44 (dd, J = 8.6, 3.6 Hz, 1H), 4.63 (t, J = 6.4 Hz, 2H), 4.37 (t, J = 8.8 Hz, 1H), 3.20 (t, J = 8.8 Hz, 2H), 2.85 (s, 3H), 2.60 (s, 3H), 2.36 (s, 3H). ^{13}C NMR (101 MHz, DMSO-d_6): δ ^{13}C NMR (101 MHz, DMSO-d_6): δ 156.9, 156.1, 154.5, 154.2, 152.2, 147.2, 143.9, 142.1, 133.3, 130.1, 129.8, 127.3, 124.7, 121.8, 121.6, 114.5, 114.2, 108.8, 108.3, 72.0, 43.8, 37.9, 29.0, 19.4, 18.7. LC−MS: $[M + H]^+$, 468.14.

*N-((5-Fluoro-2,3-dihydrobenzofuran-4-yl)methyl)-8-(2-methyl-6-(trifluoromethyl)pyridin-3-yl)-1-(methylsulfonyl)imidazo[1,5-c]-pyrimidin-5-amine (**33**).* ^{1}H NMR (400 MHz, MeOH-d_4): δ 8.93 (s, 1H), 8.79 (t, J = 5.0 Hz, 1H), 7.84 (d, J = 7.8 Hz, 1H), 7.72 (d, J = 7.9 Hz, 1H), 7.46 (s, 1H), 6.97 (dd, J = 10.3, 8.6 Hz, 1H), 6.73 (dd, J = 8.6, 3.9 Hz, 1H), 4.84−4.66 (m, 2H), 4.57 (t, J = 8.7 Hz, 2H), 3.40−3.29 (m, 2H), 3.02 (s, 3H), 2.35 (s, 3H). LC−MS: $[M + H]^+$, 522.11.

*N-((5-Fluoro-2,3-dihydrobenzofuran-4-yl)methyl)-8-(1-methyl-1H-pyrazol-4-yl)-1-(methylsulfonyl)imidazo[1,5-c]pyrimidin-5-amine (**34**).* ^{1}H NMR (400 MHz, MeOH-d_4): δ 8.63 (s, 1H), 7.76 (s, 1H), 7.59 (s, 1H), 7.44 (s, 1H), 6.85 (t, J = 9.6 Hz, 1H), 6.64 (dd, J = 8.4, 3.6 Hz, 1H), 4.81 (s, 2H), 4.57 (t, J = 8.4 Hz, 2H), 3.94 (s, 3H), 3.36 (t, J = 8.8 Hz, 2H), 3.00 (s, 3H), 2.66 (s, 2H). LC−MS: $[M + H]^+$, 443.12.

*N-((5-Fluoro-2,3-dihydrobenzofuran-4-yl)methyl)-8-(tetrahydro-2H-pyran-4-yl)imidazo[1,5-c]pyrimidin-5-amine (**59**).* 3,6-Dihydro-2*H*-pyran-4-boronic acid pinacol ester (290 mg, 1.38 mmol), $Pd(PPh_3)_4$ (80 mg, 0.069 mmol), and Na_2CO_3 (285 mg) were added to a solution (dioxane/H_2O = 10:2.5 mL) of compound **56** (250 mg, 0.69 mmol). The resulting mixture was stirred under N_2 at 90 °C overnight. The mixture was then cooled to rt, and the solvent was removed in vacuo and purified by column chromatography (eluting with 0−5% MeOH/DCM) to obtain the title compound **59** as a white solid in 80% yield. LC−MS: $[M + H]^+$, 367.14.

*N-((5-Fluoro-2,3-dihydrobenzofuran-4-yl)methyl)-8-(tetrahydro-2H-pyran-4-yl)imidazo[1,5-c]pyrimidin-5-amine (**60**).* Pd/C (100 mg, 10% wt) was added to a solution of compound **59** (1 g, 2.70 mmol) in MeOH (25 mL). The reaction mixture was degassed with H_2 and stirred under an H_2 atmosphere for 6 h at rt. The mixture was then filtered through Celite and washed with MeOH. Concentration under reduced pressure yielded the desired product. LC−MS: $[M + H]^+$, 369.17.

*N-((5-Fluoro-2,3-dihydrobenzofuran-4-yl)methyl)-1-iodo-8-(tetrahydro-2H-pyran-4-yl)imidazo[1,5-c]pyrimidin-5-amine (**61**).* NIS (82 mg, 0.4 mmol) was added at 0 °C to a solution of compound **60** (160 mg, 0.43 mmol) in DMF (4 mL) and stirred at rt for 15 min. The mixture was extracted with DCM (4 × 50 mL), washed with brine (30 mL), dried (Na_2SO_4), and filtered. The filtrate was concentrated, and the residue was purified by column chromatography (eluting with 20−50% EtOAc/hexane) to afford the title compound **61** in 60% yield (127 mg, 0.25 mmol, 70%). LC−MS: $[M + H]^+$, 495.04.

*N-((5-Fluoro-2,3-dihydrobenzofuran-4-yl)methyl)-1-(methylsulfonyl)-8-(tetrahydro-2H-pyran-4-yl)imidazo[1,5-c]pyrimidin-5-amine (**35**).* A mixture of compound **61** (50 mg, 0.1 mmol), $MeSO_2Na$ (30 mg. 0.3 mmol), and CuI (57 mg. 0.3 mmol) in DMSO (2 mL) was bubbled with N_2 for 5 min and the sealed tube was then heated in a microwave reactor at 120 °C for 20 min and then at 100 °C for 3 h. The mixture was concentrated, and the residue was purified by HPLC to afford the title compound **35** (21 mg, 0.05 mmol) in 50% yield. ^{1}H NMR (400 MHz, DMSO-d_6): δ 8.80 (s, 1H), 8.44 (t, J = 5.1 Hz, 1H), 7.49 (s, 1H), 6.94 (dd, J = 10.3, 8.7 Hz, 1H), 6.70 (dd, J = 8.7, 3.9 Hz, 1H), 4.68 (d, J = 4.4 Hz, 2H), 4.54 (t, J = 8.7 Hz, 2H), 3.95 (dd, J = 11.1, 3.8 Hz, 2H), 3.66 (ddd, J = 11.7, 8.4, 3.3 Hz, 1H), 3.40 (d, J = 1.9 Hz, 1H), 3.36 (s, 3H), 3.29 (t, J = 8.7 Hz, 2H), 1.81 (d, J = 13.6 Hz, 2H), 1.67 (qd, J = 12.3, 4.2 Hz, 2H). LC−MS: $[M + H]^+$, 447.14.

*4-(5-(((5-Fluoro-2,3-dihydrobenzofuran-4-yl)methyl)amino)-1-(methylsulfonyl)imidazo[1,5-c]pyrimidin-8-yl)tetrahydro-2H-thiopyran 1,1-Dioxide (**36**).* ^{1}H NMR (400 MHz, DMSO-d_6): δ 8.83 (s, 1H), 8.51 (t, J = 5.1 Hz, 1H), 7.54 (d, J = 0.7 Hz, 1H), 6.93 (dd, J = 10.3, 8.7 Hz, 1H), 6.70 (dd, J = 8.6, 3.9 Hz, 1H), 4.67 (d, J = 4.3 Hz, 2H), 4.55 (t, J = 8.7 Hz, 2H), 3.72−3.59 (m, 1H), 3.38 (s, 3H), 3.31 (t, J = 8.7 Hz, 2H), 3.27−3.06 (m, 4H), 2.31−2.19 (m, 2H), 2.19−2.04 (m, 2H). LC−MS: $[M + H]^+$, 495.10.

https://dx.doi.org/10.1021/acs.jmedchem.0c00479
J. Med. Chem. 2020, 63, 7252−7267

*N-((5-Fluoro-2,3-dihydrobenzofuran-4-yl)methyl)-1-(methylsulfonyl)-8-(1-(methylsulfonyl)piperidin-4-yl)imidazo[1,5-c]pyrimidin-5-amine (**37**).* ^{1}H NMR (400 MHz, DMSO-d_6): δ 8.81 (s, 1H), 8.46 (s, 1H), 7.54 (d, J = 0.7 Hz, 1H), 6.94 (dd, J = 10.3, 8.7 Hz, 1H), 6.70 (dd, J = 8.6, 3.9 Hz, 1H), 4.68 (d, J = 3.9 Hz, 2H), 4.54 (t, J = 8.7 Hz, 2H), 3.73−3.65 (m, 2H), 3.59−3.45 (m, 1H), 3.37 (s, 3H), 3.29 (t, J = 8.7 Hz, 2H), 2.91 (s, 3H), 2.76 (td, J = 12.1, 2.3 Hz, 2H), 2.00 (d, J = 12.6 Hz, 2H), 1.69 (qd, J = 12.4, 3.9 Hz, 2H). LC−MS: $[M + H]^+$, 524.13.

*8-(1-Ethylpiperidin-4-yl)-N-((5-fluoro-2,3-dihydrobenzofuran-4-yl)methyl)-1-(methylsulfonyl)imidazo[1,5-c]pyrimidin-5-amine (**38**).* ^{1}H NMR (400 MHz, DMSO-d_6): δ 8.85 (s, 1H), 8.55 (br s, 1H), 7.45 (d, J = 0.7 Hz, 1H), 6.94 (dd, J = 10.3, 8.7 Hz, 1H), 6.70 (dd, J = 8.6, 3.9 Hz, 1H), 4.69 (d, J = 2.8 Hz, 2H), 4.54 (t, J = 8.7 Hz, 2H), 3.62 (dd, J = 13.8, 10.7 Hz, 3H), 3.38 (s, 3H), 3.29 (t, J = 8.7 Hz, 2H), 3.26−3.10 (m, 2H), 2.94 (q, J = 11.2 Hz, 2H), 2.16 (d, J = 14.0 Hz, 2H), 1.87 (dd, J = 14.6, 11.2 Hz, 2H), 1.25 (t, J = 7.3 Hz, 3H). LC−MS: $[M + H]^+$, 474.18.

*1-(4-(5-(((5-Fluoro-2,3-dihydrobenzofuran-4-yl)methyl)amino)-1-(methylsulfonyl)imidazo[1,5-c]pyrimidin-8-yl)piperidin-1-yl)-ethan-1-one (**39**).* ^{1}H NMR (400 MHz, DMSO-d_6): δ 8.81 (s, 1H), 8.46 (s, 1H), 7.46 (d, J = 0.7 Hz, 1H), 6.93 (dd, J = 10.3, 8.6 Hz, 1H), 6.69 (dd, J = 8.6, 3.9 Hz, 1H), 4.67 (s, 2H), 4.54 (t, J = 8.7 Hz, 3H), 3.93 (d, J = 13.6 Hz, 1H), 3.71−3.57 (m, 1H), 3.37 (s, 3H), 3.29 (t, J = 8.7 Hz, 2H), 3.15−2.97 (m, 1H), 2.50−2.49 (m, 1H), 2.02 (s, 3H), 1.99−1.81 (m, 2H), 1.51 (dqd, J = 41.9, 12.4, 4.0 Hz, 2H). LC−MS: $[M + H]^+$, 488.16.

*8-(1-(Cyclopropylsulfonyl)piperidin-4-yl)-N-((5-fluoro-2,3-dihydrobenzofuran-4-yl)methyl)-1-(methylsulfonyl)imidazo[1,5-c]-pyrimidin-5-amine (**40**).* ^{1}H NMR (400 MHz, DMSO-d_6): δ 8.81 (s, 1H), 8.47 (s, 1H), 7.53 (d, J = 0.6 Hz, 1H), 6.93 (dd, J = 10.3, 8.7 Hz, 1H), 6.69 (dd, J = 8.6, 3.9 Hz, 1H), 4.68 (s, 2H), 4.54 (t, J = 8.7 Hz, 2H), 3.78−3.69 (m, 2H), 3.59−3.48 (m, 1H), 3.32 (s, 3H), 3.29 (t, J = 8.7 Hz, 2H), 2.88 (td, J = 12.2, 2.3 Hz, 2H), 2.71−2.60 (m, 1H), 2.00 (dd, J = 12.4, 3.1 Hz, 2H), 1.69 (qd, J = 12.5, 3.9 Hz, 2H), 1.06−0.89 (m, 4H). LC−MS: $[M + H]^+$, 550.15.

*2-Bromo-4-(2,2-diethoxyethoxy)-1-fluorobenzene (**66**).* K_2CO_3 (109 g, 0.78 mol, 3 equiv) was added in one portion to a solution of 3-bromo-4-fluoro phenol (**65**, 50 g, 0.26 mol, 1 equiv) and 2-bromo-1,1-diethoxyethane (67 g, 0.34 mol, 1.3 equiv) in 250 Ml of DMF. The suspension was heated at 110 °C and stirred overnight under N_2. After cooling to rt, the reaction was diluted with H_2O and extracted with EtOAc (2 × 500 mL). The combined organic phase was washed with brine and dried over anhydrous Na_2SO_4. The residue was purified on silica gel (0−10% EtOAc/hexane) to give the title compound **66** as a yellow oil (60.12 g, 196 mmol, 75% yield). ^{1}H NMR (400 MHz, MeOH-d_4): δ 7.13 (d, 1H), 7.04 (dd, 1H), 6.84 (dd, 1H), 4.82 (t, 1H), 3.97 (d, 2H), 3.78 (q, 2H), 3.65 (q, 2H), 1.27 (t, 6H). LC−MS: $[M + H]^+$, 307.02.

*4-Bromo-5-fluorobenzofuran (**67**) and 6-Bromo-5-fluorobenzofuran (**68**).* To a solution of PPA (132.4 g, 0.39 mol) and toluene (300 mL) was added compound **66** (100 g, 0.35 mol) for over 30 min at 100 °C. The reaction mixture was heated at 100 °C for 4 h. After cooling to rt, 400 mL of ice H_2O was added and the mixture was extracted with hexane twice. The combined organic phase was washed with brine and dried over anhydrous Na_2SO_4. The residue was purified on silica gel (0−10% EtOAc/hexane) to give the title compound **67** and **68** as a isomeric mixture in 45% overall yield. LC−MS: $[M + H]^+$, 214.94.

*5-Fluorobenzofuran-4-carbonitrile (**69**) and 5-Fluorobenzofuran-6-carbonitrile (**70**).* $Pd(PPh_3)_4$ (16.2 g, 14 mmol) was added to a solution of **67** and **68** (31 g, 0.144 mol) and $Zn(CN)_2$ (25.3 g, 0.216 mol) in 100 mL of DMF. The reaction mixture was degassed with N_2 and stirred under N_2 atmosphere for 24 h at 100 °C. After cooling to rt, H_2O was added and the mixture was extracted with EtOAc (2 × 100 mL). The combined organic phase was washed with brine and dried over anhydrous Na_2SO_4. The residue was purified on silica gel (0−20% EtOAc/hexane) to separate the desired isomer **69** as a white solid. The structure was confirmed using NMR. ^{1}H NMR (400 MHz, MeOH-d_4): δ 8.10 (dd, 1H), 7.89 (dd, 1H), 7.30 (dd, 1H), 7.07 (d, 1H). LC−MS: $[M + H]^+$, 162.02.

*(5-Fluorobenzofuran-4-yl)methanamine (**71**).* The desired isomer **69** (2.3 g, 14.55 mmol) in 10 mL of THF was treated with a 1 M solution of LAH in THF (36 mL) at 0 °C. Then, the temperature was increased to 50 °C and the reaction mixture was stirred overnight. After cooling to rt, the reaction was slowly quenched with satd. Na_2SO_4 at 0 °C. It was then filtered and washed several times with EtOAc. Purification by flash chromatography (0−10% MeOH/DCM containing 1% triethylamine) gave the desired compound **71** (1.63 g, 10.1 mmol) in 70% yield. LC−MS: $[M + H]^+$, 166.02.

*(5-Fluoro-2,3-dihydrobenzofuran-4-yl)methanamine (**72**).* Pd/C (100 mg, 10% wt) was added to a solution of compound **71** (1 g, 6.02 mmol) in MeOH (50 mL). The reaction mixture was degassed with H_2 and stirred under an H_2 atmosphere for 6 h at 40 °C. The mixture was then filtered through Celite and washed with MeOH. Concentration under reduced pressure followed by purification by flash chromatography (0−10% MeOH/DCM containing 1% triethylamine) gave the desired compound **72** (859 mg, 5.11 mmol) in 85% yield. ^{1}H NMR (400 MHz, MeOH-d_4): 6.81 (dd, 1H), 6.59 (dd, 1H), 4.56 (t, 2H), 3.77 (s, 2H), 3.27 (t, 2H). LC−MS: $[M + H]^+$, 168.07.

EED-H3K27me3 Peptide Competition Binding Assay by AlphaScreen. To assess the potency of the compounds in the EED-H3K27me3 competitive binding assay, compounds were serially diluted in DMSO to obtain a total of 12 concentrations. Then, 2.5 μL of a solution of compounds at each concentration were transferred into 384-well PerkinElmer OptiPlate-384 white plates. The solutions (5 μL) containing 20 nM EED (1-441)-His protein in the buffer (25 mM HEPES, pH 8, 0.02% Tween-20, 0.5% BSA) was added to the wells and then incubated with the compound for 15 min. The solutions (2.5 μL) containing 20 nM biotin-H3K27me3 (19−33) peptide in the buffer (25 mM HEPES, pH 8, 0.02% Tween-20, 0.5% BSA) were added to the wells and incubated with the compound for 30 min. An AlphaScreen detection beads mix was prepared immediately before use by mixing nickel chelate acceptor beads and streptavidin donor beads in a 1:1 ratio (PerkinElmer, product no. 6760619C/M/R) into the buffer described above. Then, 10 μL of the detection beads mix was added to the plate, which was then incubated in dark at rt for 1 h. The final concentration of donor and acceptor beads was 10 μg/mL in each case. Plates were read on a CLARIOStar plate reader (BMG Labtech) using the AlphaScreen setting adapted for optimal signal detection with a 615 nm filter, after sample excitation at 680 nm. The emission signal at 615 nm was used to quantify the inhibition of the compounds. AlphaScreen signals were normalized based on the reading coming from the positive (maximum signal control) and negative controls (minimum signal control) to give the percentage of activity remaining. The data were then fit to a dose−response equation to obtain the IC_{50} values.

Cell Growth Inhibition. The human B cell lymphoma cell KARPAS422 and Pfeiffer cell lines were purchased from the American Type Culture Collection (ATCC) and were cultured using standard cell culture conditions in RPMI-1640 (Invitrogen, cat #11875) supplemented with 10% FBS (Invitrogen, cat #10099-141) in a humidified incubator at 37 °C, 5% CO_2. To assess the effect of EED inhibitors on cell growth, the cells were seeded in 96-well cell culture plates at a density of 2000−3000 cells/well in 200 μL of culture medium and treated with serially diluted compounds for 7 days at 37 °C in an atmosphere of 5% CO_2. Cell growth was evaluated by a lactate dehydrogenase-based WST-8 assay (Dojindo Molecular Technologies) using a Tecan Infinite M1000 multimode microplate reader (Tecan, Morrisville, NC). The WST-8 reagent was added to the plate, incubated for 1−4 h, and read at 450 nm. The readings were normalized to the DMSO-treated cells, and the IC_{50} was calculated by nonlinear regression analysis using GraphPad Prism 6 software.

PD and Efficacy Studies in Mice. Animal experiments were performed under an approved animal protocol (Protocol ID: PRO00007499, PI: Shaomeng Wang) by the Institutional Animal Care & committee of the University of Michigan. Xenograft tumors were established by injecting 1 × 10^7 KARPAS422 human B cell lymphoma cells in 50% Matrigel subcutaneously on the dorsal side of severe combined immune-deficient (SCID) mice, obtained from Charles River, with one tumor per mouse. When tumors reached

https://dx.doi.org/10.1021/acs.jmedchem.0c00479
J. Med. Chem. 2020, 63, 7252−7267

~100 mm^3, the mice were randomly assigned to treatment and vehicle control groups. The animals were monitored daily for any signs of toxicity and weighed 2−3 times per week during the treatment period and at least weekly after the treatment ended. Tumor size was measured utilizing electronic calipers 2−3 times per week during the treatment period and at least weekly after the treatment ended. Tumor volume was calculated as $V = L \times W^2/2$, where L is the length and W is the width of the tumor. EED inhibitors were formulated as a suspension in PEG 200 and administered orally by gavage at indicated doses. When applicable, results are presented as mean ± SEM. Graphing and statistical analysis were performed using GraphPad Prism 7.00 (GraphPad Software).

For pharmacodynamic analysis, resected control and treated KARPAS422 xenograft tumor tissues were ground into powder in liquid nitrogen and lysed in CST lysis buffer with halt proteinase inhibitors. Twenty micrograms of whole tumor clarified lysates were separated on 4−20 or 4−12% Novex gels. Histone proteins were extracted from the tumor tissue with the EpiQuik Total Histone Extraction Kit, purchased from EpiGentek (#OP-0006-100, Farmingdale, NY), and the level of H3K27me3 was examined by Western blotting analysis. Total histone H3 was used as the loading control. Three mice were used for each compound with each mouse bearing one tumor. The Histone H3 (#4499) and Tri-Methyl-Histone H3(Lys27) (#9733) antibodies were purchased from Cell Signaling Technology, Inc. (Danvers, MA).

Expression and Purification of the EED Protein. The gene for human EED (residues 77−441 with M370T mutation) was cloned into the pMCSG7 vector and expressed with an N-terminal 6xHis Tag with a TEV cleavage site (His-TEV-EED). *Escherichia coli* Rosetta 2 (DE3) cells were transformed with the aforementioned vector and grown in Terrific Broth supplemented with 100 μg/mL ampicillin at 37 °C. Once cells reached an OD_{600} of 1.0, expression was induced by addition of 0.4 mM IPTG. The cells were incubated at 20 °C overnight, harvested by centrifugation at 6700*g*, and stored at −80 °C until further purification.

The protein was purified by resuspending a thawed pellet from 1 L expression media in 40 mL lysis buffer containing 25 mM Tris pH 7.5, 200 mM NaCl, 0.1% mercaptoethanol, 10 μg/mL aprotinin, and 1 μg/mL leupeptin. Cells were lysed by sonication and insoluble materials cleared from the lysate by centrifugation at 34,000*g*. The resulting supernatant was incubated with 5 mL of Ni-NTA resin at 4 °C for 1 h, then washed with buffer containing 25 mM Tris pH 7.5, 200 mM NaCl, and 10 mM imidazole. His-TEV-EED was eluted from Ni-NTA resin with 25 mL of buffer comprising 25 mM Tris pH 7.5, 200 mM NaCl, and 300 mM imidazole. The eluted protein was treated with TEV protease to remove the affinity tag and then dialyzed against 1 L of buffer containing 25 mM Tris pH 7.5, 150 mM NaCl, and 0.1% mercaptoethanol overnight. EED was further purified by size exclusion chromatography on a HiLoad 16/60 Superdex 200 column (GE Healthcare) pre-equilibrated with 25 mM Tris pH 7.5, 200 mM NaCl, and 1 mM DTT. The purified protein was dialyzed into 20 mM Tris pH 8.7, 150 mM NaCl, 1 mM TCEP, and concentrated to 4 mg/mL for crystallization.

Crystallization and Structure Determination of EED Protein in a Complex with EED Inhibitors. Human EED was crystallized by sitting drop vapor diffusion at 20 °C. Drops producing crystals contained concentrated protein (4 mg/mL in 20 mM Tris pH 8.7, 150 mM NaCl, 1 mM TCEP) mixed with an equal volume of well solution containing 100 mM Tris pH 8.5, 4.2 M sodium formate, 18% glycerol, and 10 mM tris(2-carboxyethyl)phosphine. The crystals were transferred into a soak solution consisting of well solution supplemented with 1 mM EEDi-5285 or 5 mM EEDi-1056 and incubated at 20 °C for 18−20 h and then flash-frozen in liquid nitrogen.

Diffraction data were collected on the Advanced Photon Source LS-CAT beamlines 21-ID-D or 21-ID-F (Supporting Information, Table S1), processed with HKL2000,[24] and solved by molecular replacement in Molrep[25] using a published structure of EED as a search model (PDB ID: 2QXV, chain A).[26] Iterative model building and refinement were performed using COOT[27] and BUSTER,[28] respectively. Ligand restraints were generated using GRADE.[29]

The structures of EED with inhibitors EEDi-5285 (PDB ID: 6W7F) and EEDi-1056 (PDB ID: 6W7G) were solved in $P2_12_12_1$ to 2.2 and 1.85 Å, respectively, with one chain of protein comprising the asymmetric unit. The overall structure of the EEDi-5285 and EEDi-1056 proteins was highly similar, with an rmsd of 0.3 Å based on SSM superpositioning in COOT.[27] In addition to the ligand density observed in the methyllysine binding site for each inhibitor (Figure S1A,B), electron density corresponding to each inhibitor was observed in a secondary site on the surface of the protein in their respective structures at varying degrees of occupancy (Figure S2A,B). This secondary site is lined by hydrophobic residues L205, M271, and I274, with interactions occurring between the Y277 and the [1,2,4]-triazolopyridine core of each inhibitor as well as between H199 and the dihydrobenzofuran moiety (Figure S3). Both inhibitors also participate in hydrogen bonding with D202 and interact with residues E249 and the backbone carbonyl of K275 through H_2O networks. This site is unoccupied in all available cocrystal structures of EED bound to both small molecule inhibitors as well as partner proteins making up the polycomb complex, and whether or not it modulates the function has yet to be determined.

■ ASSOCIATED CONTENT

Supporting Information

The Supporting Information is available free of charge at https://pubs.acs.org/doi/10.1021/acs.jmedchem.0c00479.

^1H NMR and ^{13}C NMR spectra of representative compounds (PDF)

Crystallography data collection and refinement statistics; difference in electron density contoured to 3σ; and molecular string files for all the final target compounds (CSV)

Accession Codes

Coordinates of cocrystal structures for compound **28** (EEDi-5285) in a complex with EED and for compound **32** (EEDi-1056) in a complex with EED have been deposited into Protein Data Bank with accession codes of 6W7F and 6W7G, respectively. Authors will release the atomic coordinates upon the publication of this article.

■ AUTHOR INFORMATION

Corresponding Author

Shaomeng Wang − *Rogel Cancer Center, Departments of Internal Medicine and Pharmacology, Medical School, and Department of Medicinal Chemistry, College of Pharmacy, University of Michigan, Ann Arbor, Michigan 48109, United States*; orcid.org/0000-0002-8782-6950; Email: shaomeng@umich.edu

Authors

Rohan Kalyan Rej − *Rogel Cancer Center and Department of Internal Medicine, University of Michigan, Ann Arbor, Michigan 48109, United States*

Changwei Wang − *Rogel Cancer Center and Department of Internal Medicine, University of Michigan, Ann Arbor, Michigan 48109, United States*

Jianfeng Lu − *Rogel Cancer Center and Department of Internal Medicine, University of Michigan, Ann Arbor, Michigan 48109, United States*

Mi Wang − *Rogel Cancer Center and Department of Internal Medicine, University of Michigan, Ann Arbor, Michigan 48109, United States*

https://dx.doi.org/10.1021/acs.jmedchem.0c00479
J. Med. Chem. 2020, 63, 7252−7267

Elyse Petrunak − *Life Sciences Institute, University of Michigan, Ann Arbor, Michigan 48109, United States*
Kaitlin P. Zawacki − *Rogel Cancer Center and Department of Internal Medicine, University of Michigan, Ann Arbor, Michigan 48109, United States*
Donna McEachern − *Rogel Cancer Center and Department of Internal Medicine, University of Michigan, Ann Arbor, Michigan 48109, United States*
Ester Fernandez-Salas − *Rogel Cancer Center and Department of Internal Medicine, University of Michigan, Ann Arbor, Michigan 48109, United States*
Chao-Yie Yang − *Rogel Cancer Center and Department of Internal Medicine, University of Michigan, Ann Arbor, Michigan 48109, United States;* orcid.org/0000-0002-5445-0109
Lu Wang − *Rogel Cancer Center and Department of Pharmaceutical Sciences, College of Pharmacy, University of Michigan, Ann Arbor, Michigan 48109, United States*
Ruiting Li − *Rogel Cancer Center and Department of Pharmaceutical Sciences, College of Pharmacy, University of Michigan, Ann Arbor, Michigan 48109, United States*
Krishnapriya Chinnaswamy − *Life Sciences Institute, University of Michigan, Ann Arbor, Michigan 48109, United States*
Bo Wen − *Rogel Cancer Center and Department of Pharmaceutical Sciences, College of Pharmacy, University of Michigan, Ann Arbor, Michigan 48109, United States*
Duxin Sun − *Rogel Cancer Center and Department of Pharmaceutical Sciences, College of Pharmacy, University of Michigan, Ann Arbor, Michigan 48109, United States;* orcid.org/0000-0002-6406-2126
Jeanne Stuckey − *Rogel Cancer Center and Life Sciences Institute, University of Michigan, Ann Arbor, Michigan 48109, United States*
Yunlong Zhou − *Ascentage Pharma Group, Suzhou, Jiangsu 215216, China*
Jianyong Chen − *Ascentage Pharma Group, Suzhou, Jiangsu 215216, China*
Guozhi Tang − *Ascentage Pharma Group, Suzhou, Jiangsu 215216, China;* orcid.org/0000-0002-7131-4678

Complete contact information is available at: https://pubs.acs.org/10.1021/acs.jmedchem.0c00479

Author Contributions

[▽]R.K.R. and C.W. contributed equally.

Notes

The authors declare the following competing financial interest(s): The University of Michigan has filed a patent application on these EED inhibitors, which has been licensed by Ascentage Pharma Group. S. Wang, R. Rej, C. Wang, M. Wang, J. Lu, C.-Y. Yang, E. Fernandez-Salas, and J. Stuckey are co-inventors on the patent application. The University of Michigan has received a research contract from Ascentage. S.W. is a co-founder of Ascentage, owns shares in Ascentage and is a paid consultant to Ascentage. The University of Michigan also owns shares in Ascentage.

■ ACKNOWLEDGMENTS

This work was supported in part by a research contract from Ascentage Pharma Group (to S.W.) and the Rogel Cancer Center Support Grant from National Cancer Institute, NIH (P30 CA046592). Use of the Advanced Photon Source, an Office of Science User Facility operated for the U.S. Department of Energy (DOE) Office of Science by Argonne National Laboratory, was supported by the U.S. DOE under contract no. DE-AC02-06CH11357. Use of the LS-CAT Sector 21 was supported by the Michigan Economic Development Corporation and the Michigan Technology Tri-Corridor (Grant 085P1000817).

■ ABBREVIATIONS

PRC, polycomb repressive complex; EED, embryonic ectoderm development; H3K27, histone 3 lysine 27; SAM, *S*-adenosylmethionine; SAH, *S*-adenosyl-L-homocysteine hydrolase; NMR, nuclear magnetic resonance; DMSO, dimethyl sulfoxide; SAR, structure−activity relationship; HPLC, high-performance liquid chromatography; PPA, polyphosphoric acid; rt, room temperature; UPLC, ultraperformance liquid chromatography; SCID mice, severe combined immunodeficient mice; CL, volume of plasma cleared of the drug per unit time; TGI, tumor growth inhibition; V_{ss}, steady-state volume of distribution

■ REFERENCES

(1) Lewis, E. B. A gene complex controlling segmentation in Drosophila. *Nature* **1978**, *276*, 565−570.
(2) Margueron, R.; Reinberg, D. The polycomb complex PRC2 and its mark in life. *Nature* **2011**, *469*, 343−349.
(3) Simon, J. A.; Kingston, R. E. Mechanisms of polycomb gene silencing: knowns and unknowns. *Nat. Rev. Mol. Cell Biol.* **2009**, *10*, 697−708.
(4) Levine, S. S.; Weiss, A.; Erdjument-Bromage, H.; Shao, Z.; Tempst, P.; Kingston, R. E. The core of the polycomb repressive complex is compositionally and functionally conserved in flies and humans. *Mol. Cell. Biol.* **2002**, *22*, 6070−6078.
(5) Dimou, A.; Dincman, T.; Evanno, E.; Gemmill, R. M.; Roche, J.; Drabkin, H. A. Epigenetics during EMT in lung cancer: EZH2 as a potential therapeutic target. *Cancer Treat. Res. Commun.* **2017**, *12*, 40−48.
(6) Cao, R.; Wang, L.; Wang, H.; Xia, L.; Erdjument-Bromage, H.; Tempst, P.; Jones, R. S.; Zhang, Y. Role of histone H3 lysine 27 methylation in polycomb-group silencing. *Science* **2002**, *298*, 1039−1043.
(7) Kuzmichev, A.; Nishioka, K.; Erdjument-Bromage, H.; Tempst, P.; Reinberg, D. Histone methyltransferase activity associated with a human multiprotein complex containing the enhancer of zeste protein. *Gene Dev.* **2002**, *16*, 2893−2905.
(8) Qi, W.; Zhao, K.; Gu, J.; Huang, Y.; Wang, Y.; Zhang, H.; Zhang, M.; Zhang, J.; Yu, Z.; Li, L.; Teng, L.; Chuai, S.; Zhang, C.; Zhao, M.; Chan, H.; Chen, Z.; Fang, D.; Fei, Q.; Feng, L.; Feng, L.; Gao, Y.; Ge, H.; Ge, X.; Li, G.; Lingel, A.; Lin, Y.; Liu, Y.; Luo, F.; Shi, M.; Wang, L.; Wang, Z.; Yu, Y.; Zeng, J.; Zeng, C.; Zhang, L.; Zhang, Q.; Zhou, S.; Oyang, C.; Atadja, P.; Li, E. An allosteric PRC2 inhibitor targeting the H3K27me3 binding pocket of EED. *Nat. Chem. Biol.* **2017**, *13*, 381−388.
(9) He, Y.; Selvaraju, S.; Curtin, M. L.; Jakob, C. G.; Zhu, H.; Comess, K. M.; Shaw, B.; The, J.; Lima-Fernandes, E.; Szewczyk, M. M.; Cheng, D.; Klinge, K. L.; Li, H.-Q.; Pliushchev, M.; Algire, M. A.; Maag, D.; Guo, J.; Dietrich, J.; Panchal, S. C.; Petros, A. M.; Sweis, R. F.; Torrent, M.; Bigelow, L. J.; Senisterra, G.; Li, F.; Kennedy, S.; Wu, Q.; Osterling, D. J.; Lindley, D. J.; Gao, W.; Galasinski, S.; Barsyte-Lovejoy, D.; Vedadi, M.; Buchanan, F. G.; Arrowsmith, C. H.; Chiang, G. G.; Sun, C.; Pappano, W. N. The EED protein-protein interaction inhibitor A-395 inactivates the PRC2 complex. *Nat. Chem. Biol.* **2017**, *13*, 389−395.
(10) Di Croce, L.; Helin, K. Transcriptional regulation by Polycomb group proteins. *Nat. Struct. Mol. Biol.* **2013**, *20*, 1147−1155.
(11) McCabe, M. T.; Ott, H. M.; Ganji, G.; Korenchuk, S.; Thompson, C.; Van Aller, G. S.; Liu, Y.; Graves, A. P.; Iii, A. D. P.; Diaz, E.; LaFrance, L. V.; Mellinger, M.; Duquenne, C.; Tian, X.; Kruger, R. G.; McHugh, C. F.; Brandt, M.; Miller, W. H.; Dhanak, D.;

Verma, S. K.; Tummino, P. J.; Creasy, C. L. EZH2 inhibition as a therapeutic strategy for lymphoma with EZH2-activating mutations. *Nature* **2012**, *492*, 108−112.
(12) Konze, K. D.; Ma, A.; Li, F.; Barsyte-Lovejoy, D.; Parton, T.; MacNevin, C. J.; Liu, F.; Gao, C.; Huang, X.-P.; Kuznetsova, E.; Rougie, M.; Jiang, A.; Pattenden, S. G.; Norris, J. L.; James, L. I.; Roth, B. L.; Brown, P. J.; Frye, S. V.; Arrowsmith, C. H.; Hahn, K. M.; Wang, G. G.; Vedadi, M.; Jin, J. An orally bioavailable chemical probe of the Lysine Methyltransferases EZH2 and EZH1. *ACS Chem. Biol.* **2013**, *8*, 1324−1334.
(13) Knutson, S. K.; Warholic, N. M.; Wigle, T. J.; Klaus, C. R.; Allain, C. J.; Raimondi, A.; Porter Scott, M.; Chesworth, R.; Moyer, M. P.; Copeland, R. A.; Richon, V. M.; Pollock, R. M.; Kuntz, K. W.; Keilhack, H. Durable tumor regression in genetically altered malignant rhabdoid tumors by inhibition of methyltransferase EZH2. *Proc. Natl. Acad. Sci. U.S.A.* **2013**, *110*, 7922−7927.
(14) Knutson, S. K.; Kawano, S.; Minoshima, Y.; Warholic, N. M.; Huang, K.-C.; Xiao, Y.; Kadowaki, T.; Uesugi, M.; Kuznetsov, G.; Kumar, N.; Wigle, T. J.; Klaus, C. R.; Allain, C. J.; Raimondi, A.; Waters, N. J.; Smith, J. J.; Porter-Scott, M.; Chesworth, R.; Moyer, M. P.; Copeland, R. A.; Richon, V. M.; Uenaka, T.; Pollock, R. M.; Kuntz, K. W.; Yokoi, A.; Keilhack, H. Selective inhibition of EZH2 by EPZ-6438 leads to potent antitumor activity in EZH2-mutant non-hodgkin lymphoma. *Mol. Cancer Ther.* **2014**, *13*, 842−854.
(15) Bisserier, M.; Wajapeyee, N. Mechanisms of resistance to EZH2 inhibitors in diffuse large B-cell lymphomas. *Blood* **2018**, *131*, 2125−2137.
(16) Lingel, A.; Sendzik, M.; Huang, Y.; Shultz, M. D.; Cantwell, J.; Dillon, M. P.; Fu, X.; Fuller, J.; Gabriel, T.; Gu, J.; Jiang, X.; Li, L.; Liang, F.; McKenna, M.; Qi, W.; Rao, W.; Sheng, X.; Shu, W.; Sutton, J.; Taft, B.; Wang, L.; Zeng, J.; Zhang, H.; Zhang, M.; Zhao, K.; Lindvall, M.; Bussiere, D. E. Structure-guided design of EED binders allosterically inhibiting the epigenetic polycomb repressive complex 2 (PRC2) methyltransferase. *J. Med. Chem.* **2017**, *60*, 415−427.
(17) Curtin, M. L.; Pliushchev, M. A.; Li, H.-Q.; Torrent, M.; Dietrich, J. D.; Jakob, C. G.; Zhu, H.; Zhao, H.; Wang, Y.; Ji, Z.; Clark, R. F.; Sarris, K. A.; Selvaraju, S.; Shaw, B.; Algire, M. A.; He, Y.; Richardson, P. L.; Sweis, R. F.; Sun, C.; Chiang, G. G.; Michaelides, M. R. SAR of amino pyrrolidines as potent and novel protein-protein interaction inhibitors of the PRC2 complex through EED binding. *Bioorg. Med. Chem. Lett.* **2017**, *27*, 1576−1583.
(18) Dong, H.; Liu, S.; Zhang, X.; Chen, S.; Kang, L.; Chen, Y.; Ma, S.; Fu, X.; Liu, Y.; Zhang, H.; Zou, B. An allosteric PRC2 inhibitor targeting EED suppresses tumor progression by modulating the immune response. *Cancer Res.* **2019**, *79*, 5587−5596.
(19) Peterson, L. A. Reactive metabolites in the biotransformation of molecules containing a furan ring. *Chem. Res. Toxicol.* **2013**, *26*, 6−25.
(20) Chan, H. M.; Fu, X.; Gu, X. J. J.; Huang, Y.; Li, L.; Mi, Y.; Qi, W.; Sendzik, M.; Sun, Y.; Wang, L.; Yu, Z.; Zhang, H.; Zhang, J. Y.; Zhang, M.; Zhang, Q.; Zhao, K. Triazolopyridine Compounds and Uses Thereof. International Patent Application PCT/IB2017/053335, WO2017221092A1, 2017, Novartis AG.
(21) Eusterwiemann, S.; Martinez, H.; Dolbier, W. R. Methyl 2,2-difluoro-2-(fluorosulfonyl)acetate, a difluorocarbene reagent with reactivity comparable to that of trimethylsilyl 2,2-difluoro-2-(fluorosulfonyl)acetate (TFDA). *J. Org. Chem.* **2012**, *77*, 5461−5464.
(22) Baskin, J. M.; Wang, Z. An efficient copper catalyst for the formation of sulfones from sulfinic acid salts and aryl iodides. *Org. Lett.* **2002**, *4*, 4423−4425.
(23) Huang, W.-S.; Liu, S.; Zou, D.; Thomas, M.; Wang, Y.; Zhou, T.; Romero, J.; Kohlmann, A.; Li, F.; Qi, J.; Cai, L.; Dwight, T. A.; Xu, Y.; Xu, R.; Dodd, R.; Toms, A.; Parillon, L.; Lu, X.; Anjum, R.; Zhang, S.; Wang, F.; Keats, J.; Wardwell, S. D.; Ning, Y.; Xu, Q.; Moran, L. E.; Mohemmad, Q. K.; Jang, H. G.; Clackson, T.; Narasimhan, N. I.; Rivera, V. M.; Zhu, X.; Dalgarno, D.; Shakespeare, W. C. Discovery of Brigatinib (AP26113), a phosphine oxide-containing, potent, orally active inhibitor of anaplastic lymphoma kinase. *J. Med. Chem.* **2016**, *59*, 4948−4964.
(24) Otwinowski, Z.; Minor, W. Processing of X-ray diffraction data collected in oscillation mode. *Methods Enzymol.* **1997**, *276*, 307−326.
(25) Vagin, A.; Teplyakov, A. MOLREP: an automated program for molecular replacement. *J. Appl. Crystallogr.* **1997**, *30*, 1022−1025.
(26) Han, Z.; Xing, X.; Hu, M.; Zhang, Y.; Liu, P.; Chai, J. Structural basis of EZH2 recognition by EED. *Structure* **2007**, *15*, 1306−1315.
(27) Emsley, P.; Lohkamp, B.; Scott, W. G.; Cowtan, K. Features and development of Coot. *Acta Crystallogr., Sect. D: Biol. Crystallogr.* **2010**, *66*, 486−501.
(28) Bricogne, G.; Blanc, E.; Brandl, M.; Flensburg, C.; Keller, P.; Paciorek, W.; Roversi, P.; Sharff, A.; Smart, O. S.; Vonrhein, C.; Womack, T. O. *BUSTER*, 2.10.3; Global Phasing Ltd.: Cambridge, United Kingdom, 2017.
(29) Smart, O. S.; Womack, T. O.; Sharff, A.; Flensburg, C.; Keller, P.; Paciorek, W.; Vonrhein, C.; Bricogne, G. *GRADE*, 1.2.13; Global Phasing Ltd.: Cambridge, United Kingdom, 2017.

https://dx.doi.org/10.1021/acs.jmedchem.0c00479
J. Med. Chem. 2020, 63, 7252−7267